Additively Manufactured Heat Exchangers

Isak Wadsö and Simon Holmqvist

DIVISION OF PRODUCT DEVELOPMENT | DEPARTMENT OF DESIGN SCIENCES
FACULTY OF ENGINEERING LTH | LUND UNIVERSITY
2020

MASTER THESIS

Additively Manufactured Heat Exchangers

Development and Testing

Isak Wadsö and Simon Holmqvist

LUND
UNIVERSITY

Additively Manufactured Heat Exchangers
Development and Testing

Published by
Department of Design Sciences
Faculty of Engineering LTH, Lund University
P.O. Box 118, SE-221 00 Lund, Sweden

Subject: Technical Design (MMKM10)
Division: Product Development
Supervisor: Axel Nordin
Co-supervisor: Martin Andersson
Examiner: Giorgos Nikoleris

Abstract

Heat exchangers are important devices in many applications. Extensive work is done in optimization, but the overall designs are often one of the conventional varieties such as plate or shell-and-tube heat exchanger. These are constrained by their manufacturing, for example the use of construction material such as sheet metal and cylindrical pipes. The current progress in additive manufacturing has the potential to disrupt convention, as it allows complex shapes better suited to the nature of fluid flow.

The intersection between heat exchangers and additive manufacturing has been explored in this thesis. The structures known as Triply Periodic Minimal Surfaces were found to have special potential because of their suitability for both heat transfer and additive manufacturing. Specifically, the "Schwarz D" and "Schoen G" varieties were used.

A method for enclosing these structures according to the internal channels was developed and a manifold was designed to allow full counter current flow. Two complete heat exchanger variations were produced in the material AlSi10Mg, evaluated experimentally and simulated using computational fluid dynamics.

This thesis suggests equal usefulness of the two proposed designs for heat exchanging applications, as well as demonstrates their manufacturability. The inner structure was found to provide good mixing and an even flow distribution, while the manifold design requires further development to lower pressure loss.

Keywords: Additive manufacturing, Heat exchanger, Triply periodic minimal surface, AlSi10Mg

Sammanfattning

Värmeväxlare är viktiga komponenter i många tillämpningar. Mycket arbete läggs på att optimera dem, men oftast begränsas den övergripande designen till någon av de konventionella varianterna såsom tub- eller plattvärmeväxlare. Tillverkningen av dessa innebär begränsningar, såsom att de tillverkas av cylindriska rör och plåt. Framsteg inom additiv tillverkning har potentialen att omkullkasta detta, då det tillåter komplexa former som är bättre lämpade för vätskors strömning.

Skärningen mellan dessa två fält har utforskats i denna rapport. "Trippelt periodiska minimala ytor" identifierades som extra intressanta på grund av deras lämpliga egenskaper för både additiv tillverkning och värmeväxling. Specifikt användes varianterna "Schwarz D" och "Schoen G".

En metod för att innesluta strukturens inre kanaler utvecklades, och en fördelare designades för att tillåta motflöde. Två kompletta varianter av värmeväxlare tillverkades i materialet AlSi10Mg och utvärderades experimentellt samt med simulering.

Denna rapport antyder likvärdig användbarhet som värmeväxlare för de två föreslagna utformningarna, och demonstrerar deras tillverkningsbarhet. Innerstrukturen erbjuder hög blandning och en jämn flödesfördelning. Fördelaren behöver dock vidareutvecklas för att reducera dess tryckförluster.

Nyckelord: Additiv tillverkning, Värmeväxlare, Trippelt periodiska minimala ytor, AlSi10Mg

Acknowledgments

Many aspects of this work were new to us, and it would not have been possible for us to reach this far without the support of the people around us. We want to specially thank our supervisors Axel Nordin and Martin Andersson, Giorgos Nikoleris for examination, Sepehr Hatami at RISE for guidance, Zan Wu for assistance with the test equipment, Johnny Nyman for help during the manufacturing and Philip Månsson for making it possible to simulate our design.

Lund, June 2020

Isak Wadsö Simon Holmqvist

Table of contents

1 Introduction

1.1 Background

Heat exchangers (HX) are used to transfer heat from one fluid to another, with the purpose of either heating or cooling. They are important devices in countless applications such as air conditioning, process industry, power generation, vehicles etc. Air, exhaust gas, water and oil are commonly used fluids. In this thesis focus is only on liquid-to-liquid HX. Conventional HX are optimized to their respective use cases, but within the boundaries of the manufacturing methods used. The starting material is most often pipes or sheet metal, and joining techniques such as welding, brazing or bolting has to be considered. A deeper look into heat exchangers can be found in section 3.2.

With additive manufacturing (AM) on the other hand, complex geometries that have previously been impossible to realize can be made in a single piece. The price to manufacture with AM is high and the manufacturable size is limited, but other aspects of value are added. Production on demand is possible, reducing the need to keep stock, and no tooling is needed. The cost is associated with volume, not shape, opening up for ways to increase value through customization and complexity. Currently AM is reserved for demanding applications such as aviation, but with more capable technology and lower prices this field is rapidly expanding, and making full use of the possibilities with AM is still an open question [1, pp. 7-8].

The interaction between the fields of HX and AM is explored in this thesis, with the goal to find geometries that provide improved heat transfer. The aim is not to optimize for a specific application, but to take a step back and examine the general possibilities when redefining the constraints. The goal is to develop a complete HX design instead of looking at a specific aspect, adding to the knowledge from which further development can be made.

1.1.1 **ReLed-3D**

This thesis was announced within the project "ReLed-3D, Resource efficient flexible production in the automotive industry through additive metal manufacturing", funded by VINNOVA FFI – Strategic Vehicle Research and Innovation. It is a multifaceted project in collaboration with partners from both

universities and industry. Previous findings such as generated concepts, test results, print parameters etc. were available for this thesis.

The demonstration part for ReLed-3D is an oil cooler in a Volvo truck, but the goals for this thesis developed to be of a more general nature.

1.2 Objective

The objective of this project is to explore the design possibilities of aluminium AM heat exchangers. It has a vision to find interdisciplinary connections and will use a rapid prototyping approach (Think-Try-Change). It aims to fulfill the goals of the ReLed-3D project: Improved efficiency through reduction in size and weight compared to a conventional HX. Utilizing the full potential of AM to integrate aspects of application beyond heat transfer is also of interest. Showing an example of a full HX made with AM is a contribution to this emerging field of research, even without improvements in thermal performance. Due to the interest and education of the authors, focus will be on 3D modelling. See Appendix A for original project plan and Appendix B for a revised version.

The project will consist of two main parts:

1. Geometries will be explored and developed. Samples will be manufactured.
2. The samples will be experimentally tested. Pressure drop and temperature difference will be measured during operation.

1.3 Delimitations

Explorations are limited to the study of two liquid flows. The study is limited to geometries suitable for AM in aluminium, in the size range possible to manufacture with the available equipment. The macro and meso geometries are explored, while study of the micro geometry and surface properties are outside the scope. Optimization of the geometry is considered outside the scope.

During the course of this project the COVID-19 pandemic broke out. This external factor limited the project but was not critical. Consultations with supervisor Axel Nordin were moved online, workshop access was somewhat limited and the technical transition from office work to working from home pushed the timeline forward. External connections were harder to establish than predicted. For example a collaboration with Alfa Laval was planned, but cancelled.

1.4 Deliverables

The deliverables of this project are this thesis, a presentation, manufactured prototypes and 3D models.

1.5 Structure of thesis

In Chapter 2 you will find descriptions of methods used during the project in regard to design process and resources used to accomplish results for modeling, manufacturing and experiment.

Chapter 3 gives an overview of theory, regarding relevant principles of physics and some specifics of HX, AM as well as previous work.

In Chapter 4, the steps taken in concept generation are shown. Concept direction stems from a summary of the results of the theory study. The basis of concept selection and can be read in Chapter 5.

Chapter 6 shows the realization of the concept, i.e. the steps taken from concept to printable 3D model. The actual manufacturing is then described in Chapter 7.

Details of experiment design and setup, as well as simulation settings are found in Chapter 0.

Chapter 9 shows the finished 3D models, the printed parts, data obtained from experiments and the simulation results showing fluid dynamic properties of the parts.

Discussions regarding the project and results are written in Chapter 10, followed by conclusions drawn and suggestions for further research and development in Chapter 11.

2 Method

This chapter describes the methods used during the project, in a general manner. Specifics are also found later in the report.

The project aims to follow the double diamond design process, whose steps are listed below [2]:

1. Clarifying objective and delimitations
2. Information gathering
3. New brief
4. Concept generation
5. Prototyping
6. Concept selection
7. Realization
8. Concept evaluation
9. Delivery of results.

Figure 2.1 shows how the phases of the project relate to the double diamond structure.

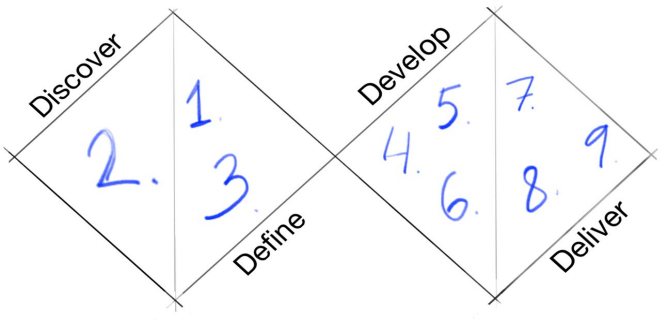

Figure 2.1 Double diamond design process, with project specific phases

The same structure is also applied locally within some of the individual phases of the project. For example the development of the testing procedure has in itself a structure similar to the whole project. Many of the steps had an iterative approach.

2.1 Information Gathering

Information about the state of research was gathered through published articles available through LUbsearch. Books were used to gather information about the more established aspects of the field. Internal documentation and a visit at the RISE facility in Mölndal provided information about the work previously done in ReLed-3D. Information was also gathered from conversations with experts.

2.2 Concept generation

Concept generation is performed to propose new or improved solutions to an existing problem or brief. The five-step method described by Ulrich and Eppinger [3, pp. 119-140] structures the process of concept generation in the following way

1. Clarify the problem
2. Search externally
3. Search internally
4. Explore systematically
5. Reflect on solution and the process

Below are the methods used for each step of concept generation.

2.2.1 **Clarify the problem**

2.2.1.1 Theory study

Books and articles on the subject are read and key information is consolidated and interpreted, keeping it relevant to the problem.

Note: for this thesis, theory and problem decomposition is closely related. In 4.4 a type of functional decomposition can be found.

2.2.2 **Search externally**

Continually ongoing process where existing solutions are studied. It's also a way to expand the horizons of the project to then focus on promising directions

2.2.2.1 Consult experts

Experts can be consulted for direct input or redirecting to fruitful areas thanks to their grasp of the field. By contacting professors, authors of articles etc. valuable time savings can be made by avoiding reinvention of the wheel.

2.2.2.2 Literature study

Searching for books and articles, products etc. to find existing solutions. By using structured databases for Internet searches, many relevant articles can be found. Good keyword usage will determine success in finding a manageable number of articles while still getting enough coverage

2.2.3 **Search internally**

2.2.3.1 Brainstorming

Brainstorming can bring new ideas to a project. Each generated idea has the chance to spark another. This exercise can be done in group or alone. The method centers on a simple statement or question and each participant writes down their associations to that statement/question.

2.2.3.2 Individual Concept Generation

In a group project each individual spends time without outside influence to generate concepts. These are presented to group members and discussed and improved.

2.2.4 **Explore systematically**

When internal and external search has been performed, there are supposedly many concepts to combine. By organizing these it allows a team to focus on the most important ones.

2.2.4.1 Concept classification tree

By dividing the solutions into distinct groups, it becomes easier to focus efforts into promising concepts. Branches are pruned when they are deemed inferior.

2.2.5 **Reflect on solution and process**

Throughout the concept generation team members should ask themselves if there are alternate approaches to the problems or the methods above that have not been explored. This helps with either reevaluating focus or solidifying decisions.

2.3 Prototyping

Creating early, simple representations of concepts will show oversights and room for improvements. This can be done with a variety of techniques and at different fidelity levels. The following prototyping techniques were used.

2.3.1 **Sketching**

Pen and paper sketches which can communicate ideas and concepts effectively to team members.

2.3.2 **Clay sculpts**

A prototyping method that shows the 3D form and its characteristics. It gives a sense of size and cutting the clay can reveal cross sections that would be hard to imagine.

2.3.3 **3D-printing**

Plastic 3D printing can produce shapes and geometries that are hard or impossible to model with clay, allowing for analysis of complex shapes. A cheap technique such as fused filament fabrication should be used when producing prototypes for early study of form/basic function. Selective laser sintering can be used when higher quality in required. More on 3D-printing and AM can be found in sections 3.3 and 3.4.

2.4 Concept selection

To narrow down which candidates to move forward with for final refinement and production, a well-informed decision needs to be made. This is done with a concept scoring matrix for this project [3, pp. 154-157].

A concept scoring matrix needs a set of criteria. Choice and weighting of these are informed by previous work done in the project. A rating scale is set, and a reference concept is chosen for which each criterion is scored as the middle ground. Going through each criterion, all concepts are scored in comparison to the reference. Then their weighted scores are added and compared. The concepts are ranked depending on score. Then concepts are, if possible, combined and improved. By varying weighting, the scoring matrix can be tested for sensitivity through repeated sessions. When a final winner is crowned, it is important to reflect on the choice as this can be a gate from which one will not iterate.

2.5 Realization

The most promising concepts will be modeled in Grasshopper (GH) and manufactured with selective laser melting (SLM) in aluminium.

2.6 Concept evaluation

When the most promising concepts have been developed and manufactured, their performance needs to be evaluated. Below are the methods used to achieve this.

2.6.1 **Experiment**

To empirically determine effectiveness of the HX design, experiments were performed. The empirical data was recorded and consolidated in graphs and tables. Through experiments it is possible to confirm or refute hypotheses regarding the function of the HX. It is also possible to compare our results to others as well as simulated results of the HX 3D model. Specifics on design of experiment and procedure is found in Chapter 0.

2.6.2 **Simulation**

An imitation of a real system can be done computationally. Input data needs to be representative of the real system for a simulation to be indicative of expected outputs of the system. With a 3D model, simulation software and reasonable inputs one can approximate the performance of a given design making it a powerful tool to inform design decisions. In combination with experiment results, the simulation can be verified and thus can help approximate unmeasured quantities. See Section 8.5 for project specifics regarding simulation.

2.7 Delivery

Methods, processes and results are recorded throughout the project and consolidated in this thesis. It describes the steps taken and reasoning behind decisions and forms the basis for the presentation held at the end of this project. The GH scripts that generate 3D models, as well as the manufactured prototypes, are also deliverables of this project.

2.8 Time plan

A plan was established that maps out the project's phases and checkpoints. The plan is not meant to be static, but a tool to guide the work. It was subject to change as the project progressed. A Gantt charts illustrating the original time plan is given in Appendix C. Details of the changes that happened to the time plan during the project can be found in Section 10.7.

2.9 Resources

2.9.1 **Grasshopper**

GH is a visual programming language integrated with the 3D modelling software Rhinoceros [4]. It is primarily used for generative algorithms and was used extensively in this project. If nothing else is stated, all 3D models shown in this report is produced by the authors in GH.

2.9.2 **ProX DMP 320**

The AM machine available to this project is a ProX DMP from 3D-Systems [5]. It is a SLM machine with a build volume of 275mm x 275mm x 420mm and uses a layer height of 30 μm.

3 Theory

This chapter describes the foundation from which concept generation and development originates. Well-established knowledge like heat transfer theory, best practices formed around AM, as well as the previous research in this field are presented.

3.1 Heat transfer

Bengt Sundén writes about the following aspects of heat transfer in the book *Introduction to heat transfer* [6].

3.1.1 **Conduction**

Within a material, heat flows from regions of higher temperature to regions of lower temperature through conduction. This is the passive process which enables the function of a HX. The heat flux increases with the temperature difference, the thermal conduction of the material and the area on which the heat transfer is occurring. Heat flux decreases with the distance the heat has to travel [6, p. 3].

3.1.2 **Convection**

Convection is the heat transport within a fluid caused by molecular heat conduction and transport of internal energy due to macroscopic movement of the fluid [6, p. 83].

Convection can be forced or natural. The former is when convection is caused by external means and the latter happens when motion is driven by inequality of densities. In the situation where the fluid motion is driven e.g. by a pump, convection is forced.

3.1.3 **Turbulence**

Flows fields are classified as either laminar or turbulent. A laminar flow field has smooth flow paths that do not cross each other. At a certain point when the velocity is increased the flow will transition from laminar to turbulent flow. In Figure 3.1 the laminar and turbulent case is shown. A turbulent flow is characterized by [6, pp. 133-134]:

- An unsteady flow field, with irregular fluid motion in time and space.
- The flow field has a high eddy activity.
- Diffusivity meaning that velocity fluctuations are spread through surrounding fluid. This implies increased heat transfer.

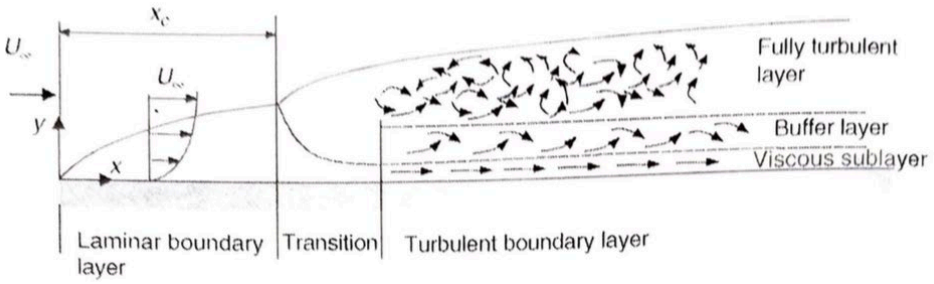

Figure 3.1 Depiction of laminar and turbulent boundary layer [6, p. 94].

The Reynold's number predicts when flows transition from laminar to turbulent. For pipe flows the Reynold's number depends on the viscosity of the fluid, the velocity and the geometry of the pipe itself. Surface roughness will also affect when transition occurs, where a rougher surface will cause earlier transition. [6, pp. 93-94]

Generally turbulent flows have greater convection [6, p. 117]. Because the no-slip condition is true at the interface between a heat conducting body and a moving fluid, heat transfer is only happening through conduction at this interface. Turbulence introduces eddy currents that transport already heated fluid away from the surface of the heat conducting body.

3.1.3.1 Viscosity

Viscosity is a physical property of fluids which describes the resistance to deformation. Viscosity can be expressed as dynamic, μ, or kinematic, ν, where $\nu = \mu/\rho$, ρ is density.

Dynamic viscosity is the resistance to deformation when external forces are of concern i.e. how much force is needed to maintain a certain flow rate. Kinematic viscosity describes how fast momentum is lost in the fluid. The viscosity of a fluid is dependent on its temperature.

3.1.4 **Overall heat transfer coefficient**

Describing the heat transfer coefficient of a HX will have to consider the variation across the whole HX. The overall heat transfer coefficient is the physical quantity that accomplishes this. It describes how effectively heat transfer occurs for a given temperature difference and it is defined by the following equation:

$$\boldsymbol{U} = \frac{\dot{Q}}{A \cdot \Delta t_m} \tag{3.1}$$

Where U is the overall heat transfer coefficient, $\dot{Q}$ is the heat transfer rate, A is the area the heat is passing and Δt_m is the logarithmic mean temperature difference.

3.1.4.1 Logarithmic Mean Temperature Difference

In the case of a counterflow HX, equation 3.2 describes the logarithmic mean temperature:

$$\Delta t_m = \mathbf{LMTD} = \frac{(t_{h,out} - t_{c,in}) - (t_{h,in} - t_{c,out})}{\ln\left(\frac{t_{h,out} - t_{c,in}}{t_{h,in} - t_{c,out}}\right)} \tag{3.2}$$

The value of the logarithmic mean temperature difference describes the heat transfer driving force.

3.2 Heat exchangers

The general characteristic of a heat exchanger is its ability to transfer heat between two or more fluids. Their application can be both cooling and heating of a medium.

3.2.1 **Compactness**

Compactness is a classification of HXs, the ratio between heat transfer area and volume determines compactness $\frac{Area}{Volume}$ of 700 m^2/m^3 or above is considered compact. [6, p. 265]

3.2.2 **Flow configurations**

Consider a finite volume unit in a flow, moving through a heat exchanger. As this volume unit travels through the channel, its temperature will change. This heat exchange is smaller or larger depending on the temperature difference compared to the fluids in the bordering channels at the volume units' current position. A bigger

difference leads to a greater heat exchange driving force. Each flow will have a mean temperature distribution from the inlet to the outlet. How this gradient interface with the gradient of the other flow affects the total heat transfer.

With this in mind, it is clear that flow configuration will affect the overall heat transfer. The main configuration of a HX classifies the system but several configurations can be present if one zooms in on certain parts of the system.

3.2.2.1 Cocurrent flow

A flow where the fluids have the same flow direction is referred to as parallel or cocurrent flow. The fluid in the channels transfer heat with a steadily decreasing temperature difference (the average temperature difference becomes low), which leads to a reduced heat transfer driving force across the length of the channels. This is depicted in Figure 3.2 (top).

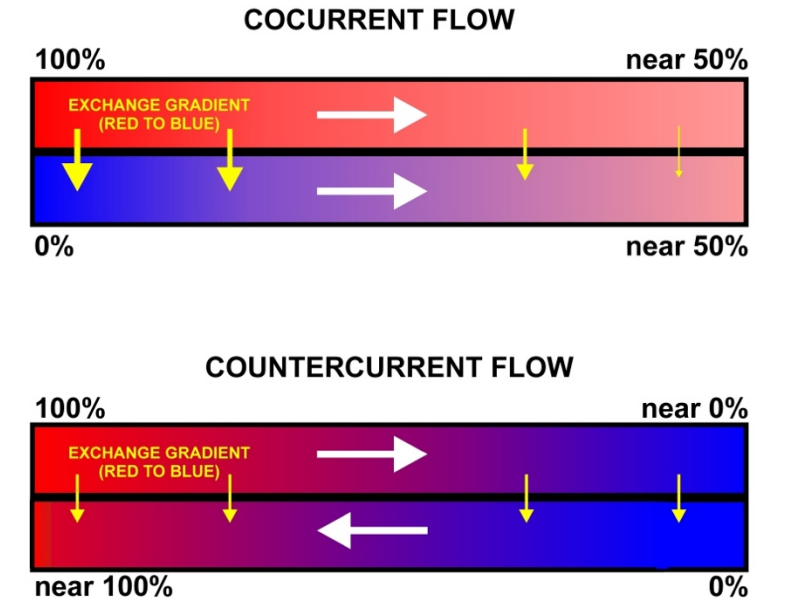

Figure 3.2 Cocurrent and countercurrent flow and corresponding exchange gradients, courtesy of Cruithne9[1]

3.2.2.2 Countercurrent flow

Flows where the fluids have opposite flow directions is referred to as countercurrent flow. In this configuration the heat transfer driving force is the highest because the

[1] CC BY-SA 4.0: https://creativecommons.org/licenses/by-sa/4.0/legalcode

average temperature difference is as high as possible. For an infinite length pipe and no heat loss to surroundings, countercurrent configuration can achieve almost complete transfer of heat. The once hot fluid would exit at nearly the same temperature as the cold inlet temperature and vice versa.

3.2.2.3 Cross flow and mixing

When a heat exchanger is designed with channels that are not parallel with respect to each other, the flow is called cross flow. This configuration can be achieved in many ways, e.g. perpendicular channels, spiral channels etc. A cross flow can be mixed or unmixed. Consider an arrangement of horizontal tubes with water flowing through, surrounded by air, free to move across the tubes. The water channels are unmixed, as the flow is never in a transversal direction relative to the tubes. The air is mixed as it is free to move in the transversal direction relative to its initial flow direction. A cross flow can also have two unmixed flows, as is the case in some plate fin HX which is described in section 3.2.3.2.

3.2.3 **Heat exchanger types**

3.2.3.1 Plate Heat Exchanger

Plate HX offer efficient heat exchange [6, p. 292]. It consists of stacked thin metal plates, sealed at the edges by elastomer gasket, brazing or welding. The seal alternates in-between plates, making a flow enter or pass the space between two given plates. This means that every other fluid channel is for one flow, and the remaining channels are reserved for the other flow as seen in Figure 3.3. The metal plates are corrugated which increases surface area and promote mixing.

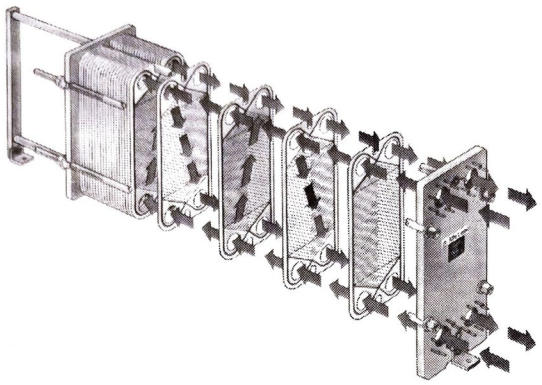

Figure 3.3 Plate Heat Exchanger [6, p. 267]

3.2.3.2 Plate Fin Heat Exchanger

A plate fin heat exchanger is typically made of alternating corrugated and flat sheets of aluminium alloys (typically), see Figure 3.4. Sides parallel with fluid flow

direction are sealed to prevent leakage. The corrugated sheets refer to the “Fin” part of the name, which extends the heat transfer area when brazed to the flat sheets and improves structural integrity. The corrugated plates can be arranged with parallel or perpendicular flow directions with respect to each other. The former can be used for cocurrent and counter-current flows and the latter is used for unmixed cross flow.

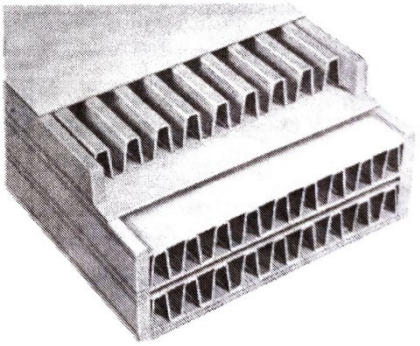

Figure 3.4 Example of Plate Fin HX [6, p. 267]

3.2.3.3 Shell and Tube Heat Exchanger

The shell and tube HX has an arrangement of tubes inside a larger container (shell). The tubes are filled with a heat exchanging media and around them another media is flowing, thus achieving heat exchange. The flow configuration across the tubes is mainly cross flow [6, p. 266]. The media in the pipes is unmixed and the surrounding media is mixed. To; promote turbulence, support the tubes, and ensure cross flow protruding baffles are mounted on the shell walls, see Figure 3.5.

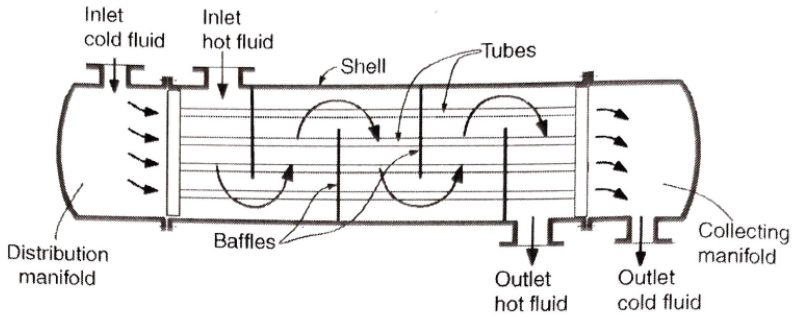

Figure 3.5 Shell and Tube heat exchanger [6, p. 266]

3.3 Additive manufacturing

3D-printing usually refers to lower-end processes, often in plastic, and additive manufacturing often refers to higher-end industrial processes, often with metal [7].

3.3.1 **Selective laser melting**

The manufacturer of the machine used in this project, ProX DMP 320, states that it use Direct Metal Printing [8]. It works according to SLM [9] and that is the term that will be used onwards in this work.

SLM builds the parts layer by layer, starting from a build plate. A scraper or roller spread metal powder over the build volume before one or more laser beams selectively bond powder particles together. Another layer is applied, and the process is repeated until the whole part is manufactured. Supports are produced at the same time, to dissipate heat and physically prevent the parts from warping and moving. To avoid oxidation the printing is done in a low pressure argon atmosphere. This enables the use of reactive metals, such as aluminium.

Compared to other metal AM processes, like Binder Jet, more post processing is necessary for SLM [1, pp. 181-182]. Support removal and surface finishing can account for a substantial part of the total part cost.

This method produces high density parts directly from the machine, but some porosity is present in SLM parts. This can be decreased with thermal treatment [10].

3.3.2 **AlSi10Mg**

The material used in this project is the aluminium alloy AlSi10Mg, manufactured by Carpenter Additive. It is originally a casting alloy with a composition close to the eutectic point of 12.6% silicon, see Figure 3.6 Al-Si Phase diagram [11]. This gives a narrow solidification range which allows for tight dimensional control when used in SLM [12]. It is light, strong and has good thermal conductivity. The addition of silicon bolsters fatigue and corrosion resistance, and magnesium increases mechanical strength.

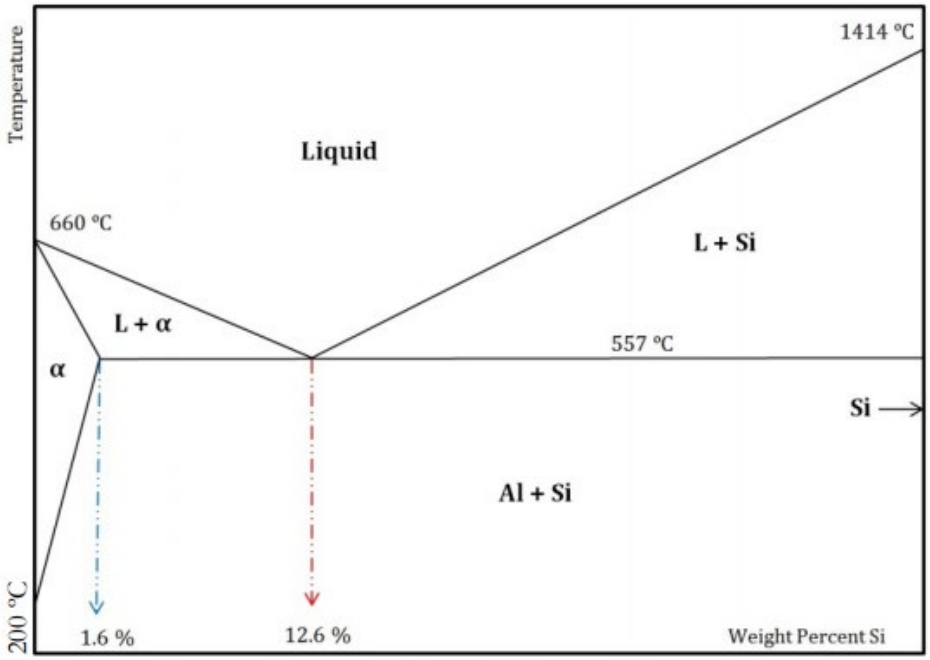

Figure 3.6 Al-Si Phase diagram

3.3.3 **Thermal treatment**

To enhance the properties of aluminium, solution heat treating and precipitation hardening can be used. The material is heated to a temperature close to its melting point for a period long enough to dissolve the alloying elements into a solid solution with the aluminium. Quenching locks the material in this state. This treatment is called T4. Aging at elevated temperature allows the oversaturated alloying atoms to migrate into balanced precipitations in an equilibrium aluminium phase, reducing lattice strain and improving strength. This is called T6.

The localized melting involved in SLM causes rapid solidification which results in properties similar to that of a T4 quenched part. It is therefore common in the industry to only do a two hour 250-300°C thermal treatment and not a full T6 cycle [13]. This relieves internal stresses and makes the material substantially less brittle. It also increase corrosion resistance and thermal conductivity [14]. To avoid warping, thermal treatment is usually done before the parts are removed from the build plate.

AlSi10Mg forms a unique structure where the Mg and Si atoms are trapped in two different micro segregated non-equilibrium phases when used in AM [15]. The cells of this structure are elongated in the build direction. Since disturbances in the crystal

structure add thermal resistance, the cell boundaries make this phenomena result in a lower thermal conductivity in the x- and y-direction in the as-built condition. Mechanical properties are also reported to be un-isotropic because of this. Heat treatment up to 350 °C makes the properties of the material gradually more isotropic and increases the thermal conductivity with as much as 75%, from around 85 to 150 W/m K [15].

3.4 Design for AM

Every manufacturing method comes with its own set of limitations and possibilities. Design for additive manufacturing (DfAM) is the concept of taking advantage of the AM process' capabilities [1, p. 41]. While AM grants a great freedom of form, it has its set of guidelines. As a branch of AM, SLM has its own characteristic consequences of not following those guidelines and has some additional design principles because of the need of heat transfer through the part into the build plate.

Nomenclature used in this section is described in Figure 3.7

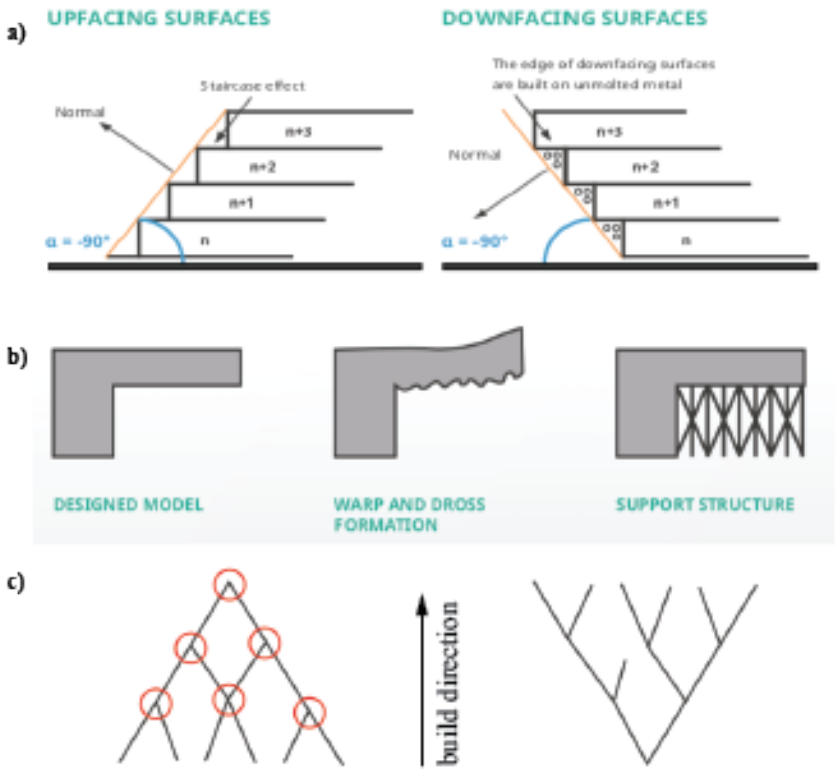

Figure 3.7 a) Definition of upwards facing and downwards facing surface for use in this thesis, b) Model with overhang, consequence in print and support solution, c) red circles mark converging points, right side shows diverging design/orientation. Courtesy of 3D systems

3.4.1 **Wall thickness**

The wall thickness of a part designed for AM should be uniform throughout. When wall thickness varies, stress concentrations can occur. Parts become vulnerable to fatigue cracks at the stress concentrations. A common method to avoid this is using fillets.

Another problem that arises from uneven wall thickness is residual stresses which are caused by rapid heating and cooling. This is the most noticeable in layers with a big cross section area. Residual stresses can be large enough to separate parts from the build plate and even cracking the entire part [1, p. 143]. By using topology optimization to remove bulky features, redesigning with even wall thickness in mind and avoiding big changes in cross sections along print direction it is possible to

avoid unwanted residual stresses. A higher number of smaller cross sections are preferable to one large cross section [8].

3.4.2 **Orientation**

Since there is anisotropy inherent in the process of SLM, the design should account for this. The build direction is the most characteristic source of anisotropy. Designs made for AM need to be able to print in at least one orientation. Besides structural integrity orientation will affect supports, heat transfer, surface finish, and build time. Listed below are some causes and effects of orienting the part in certain ways.

- One can avoid support material on a surface by tilting it away from the build plate until a self-supporting angle is reached [1, pp. 137-138].
- By flipping the part, overhangs can be avoided as the surface in question will become up facing surfaces [8].
- Heat transfer can be promoted by making sure that a large cross section is close to the build plate [8].
- Orienting the design in a way that reduces the size of cross sections normal to build direction will also reduce thermal stress [1, pp. 139-140].
- A converging geometry can be oriented in a way that makes it diverging which will eliminate shrink lines (See Figure 3.7 for clarification) [8].
- Any orientation that increases the layer count will increase the build time. [1, p. 140].

3.4.3 **Support structures**

For SLM the supports serve a dual purpose. As mentioned above, they need to support the part and dissipate heat away from the melted layer.

As the supports are needed, designs should take them into consideration from the very start. Note that adding more support will also increase build time since the laser will have a longer travel path for each layer where there's support structure.

Some of the problems that arise from poor support are listed below.

- The part could start moving from the force of the new powder layer being applied which might eventually cause failure [1, pp. 138,152].
- Residual stresses can cause warping which could lead to build failure. By adding support, more heat is transferred to the build plate. The warping

forces are counteracted by the supports and lessened by the heat transfer [1, pp. 138-139, 144].

- Unsupported surfaces with overhang will have a rough surface since the melt pool can sink into the powder bed and fuse with loose powder underneath [8].
- Regions of a cross section that are in no way connected to previously melted powder and have no support structure will create metal beads to which the next layer will fuse. This becomes a snowballing problem and can cause build failure.

With the need of support and the consequences of insufficient support established, the guidelines to avoid problems include:

- Designing with support removal in mind. If support is needed where it can't be removed, it is important that the support does not affect the function of the part [1, p. 47].
- For overhang surfaces where supports are undesirable, avoid angles below 45° away from the build plate (horizontal), doing this makes the surface self-supporting [8] [1, p. 141].
- Reduce cross section area by design or orientation to minimize warping, thereby reducing support needed [8].
- Horizontal holes with inner diameter < 8 mm will not need support [8].

3.4.4 **Weight reduction**

Reducing weight of a design meant for AM will also reduce build time and material use which both contribute to lowered costs. Lattice structures are one way to achieve this as they will reduce weight while retaining strength [1, pp. 137-138].

3.4.5 **Powder extraction**

Any enclosed volume in a design that will be produced through SLM will contain the un-melted powder caught inside as the part is built. Powder that isn't removed from said volume can be considered wasted. This is avoided by designing holes or channels through which the powder can escape. Escape channels should not be less than 0.5 mm in diameter for effective powder removal although channel and cross section shape can affect minimum powder extraction diameter. [16]

3.4.6 **Unique possibilities**

Because AM is quite costly, it is important to not only follow the above mentioned guidelines, but also to add features specifically suited to AM to gain full value from the process. Small and large features can be integrated in a single monolithic part without fasteners or seams. Variation and customization of features within a part or between parts is possible without any added printing effort. Organic shapes resulting from optimization, as well as surface patterns and lattice structures can be integrated.

3.5 Volumetric Modeling

Boundary Representations (BRep) are a common way for computer-aided design software to build 3D features. A solid and a non-solid is separated by the boundary. A BRep is composed of surfaces, curves and points.

Conversely, volumetric modeling is centered on the manipulation of voxels. A voxel is a volume element, the quick description in layman terms is “A voxel is a 3D pixel”.

When modeling in a volumetric environment one defines a space which voxels may populate, the *distance field*. Geometries are described with *distance functions*. The distance function will return a value of 0 for a point on the surface of the geometry. For points inside the geometry the function will return a negative value and for points outside the geometry a positive value is returned.

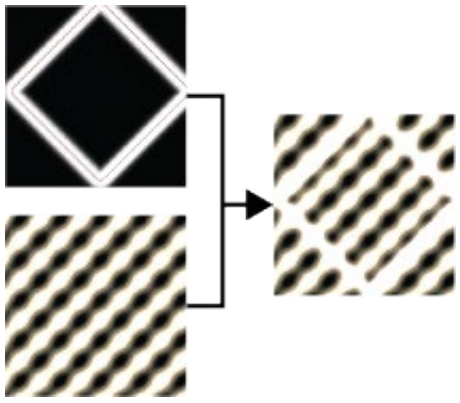

Figure 3.8 Distance functions interacting

Now consider several geometries within the distance field, their intersection will be purely a question of arithmetic, making Boolean operations fast [17]. An example of two distance functions interacting can be seen in Figure 3.8.

3.6 Previous work in ReLed-3D

The brief of this project was sprung from work done in ReLed-3D and is a continuation of the Master thesis done by Johannes Ljungman [16]. Results and conclusions from these have informed decisions made in this project.

3.6.1 **ReLed-3D**

Insight into rejected and pursued concepts, and results of measurements were relayed to this project. Concepts were focused on increasing efficiency of HXs through the benefits of AM. Test results showed the effect on pressure drop and heat transfer due to surface finish, meso structure and material. Test tubes had a single fluid channel. A takeaway for this project was that AlSi10Mg AM surfaces in an as-printed, "raw" condition were shown to improve heat transfer.

3.6.2 **3D-Printed Heat Exchanger**

The thesis that this project is a continuation of explores the design of a shell-and-tube HX for AM (see Figure 3.9), and limitations of AM with regards to narrow tube passages. Ljungman's findings affected decisions regarding minimum wall thickness and inspired the pursuit of organic designs as mentioned in Ljungman's suggestions for future work.

Figure 3.9 Shell-and-tube for AM [16]

3.7 State of the art

The field of metal AM HX is rapidly expanding [18] and is being continuously investigated. Much research is being done in academia but also in industry [19]. Below are presented applications that are interesting for this project, in the field of HX and AM.

3.7.1 **Direct replacement**

Directly translating current geometries to AM aims to demonstrate the application of AM products and its capabilities. It can also aim to lower cost, lead times and part count, and the need to keep spare parts and tools in stock.

One example is an oil cooler for an excavator being directly replaced with AM, shown in Figure 3.10. Some modifications were made to adjust for constraints involved in possible feature size and print orientation. It measured 430mm x 530mm x 50mm, showing that relatively large parts can be made. All components, including in- and outlets, were fabricated as one consolidated part. Performance is reported to be comparable to the stock HX, but lower than estimations from computational fluid dynamics (CFD) simulations. This is attributed to the problems with removing un-sintered powder from the internal channels [20].

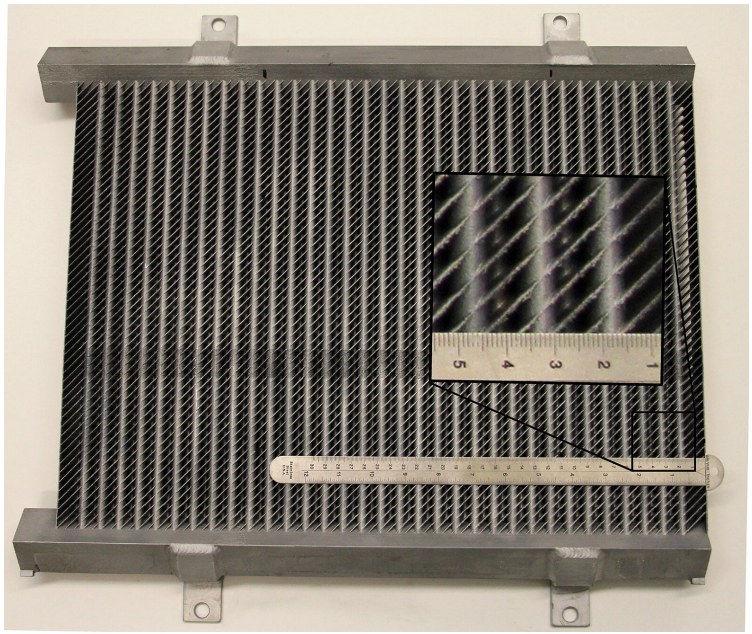

Figure 3.10 oil cooler for excavator [20]

3.7.2 **Biomimicry**

Because of the many heat and mass transfer phenomena found in nature, biomimicry has been proposed as a suitable design path for HX [21]. Blood vessels, respiratory systems and vascular systems have been evolved to favor high heat and mass transfer, and low pressure losses. They often have a fractal structure, meaning that their appearance repeats when viewed at different scales. Structures with this behavior have been found to be a very efficient way to distribute a flow from one point to a volume [22].

These tree-like structures have been investigated in the development of one-flow heat sinks for the cooling of electronics, like the examples in Figure 3.11 [23]. These findings might be integrated in a two-flow HX

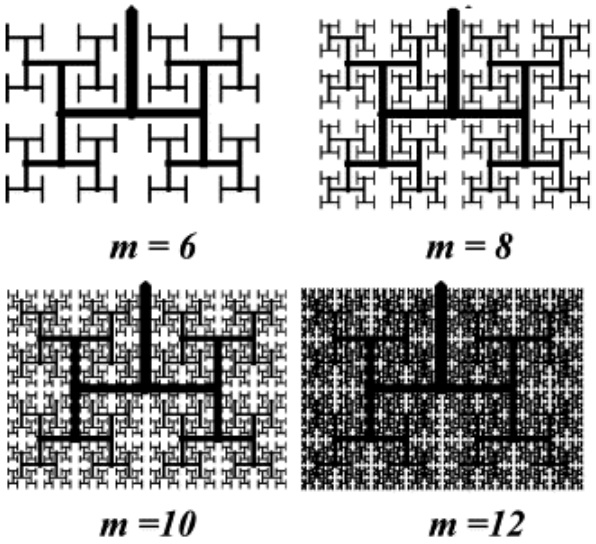

Figure 3.11 Fractal heat sinks, *m* denotes the number of pattern repetitions [23]

Branching structures in plants were studied during the design process of the inlet and outlet manifold in the variation of a shell-and-tube HX depicted in Figure 3.12 [18]. CFD was used to evaluate variations of the concept, giving valuable information before the final concept was chosen. It was found that an even and well distributed flow was easy to achieve in the inner flow, but that the surrounding flow often had a disturbed and uneven character. The relative influence of the inlet was found to be lower if the tubes in the middle section were longer (see case 3 in Figure 3.12). Constant pipe profiles were used along the whole length of the HX, but since AM was used, complicated sections could be used in order to increase heat transfer without increasing friction losses too much.

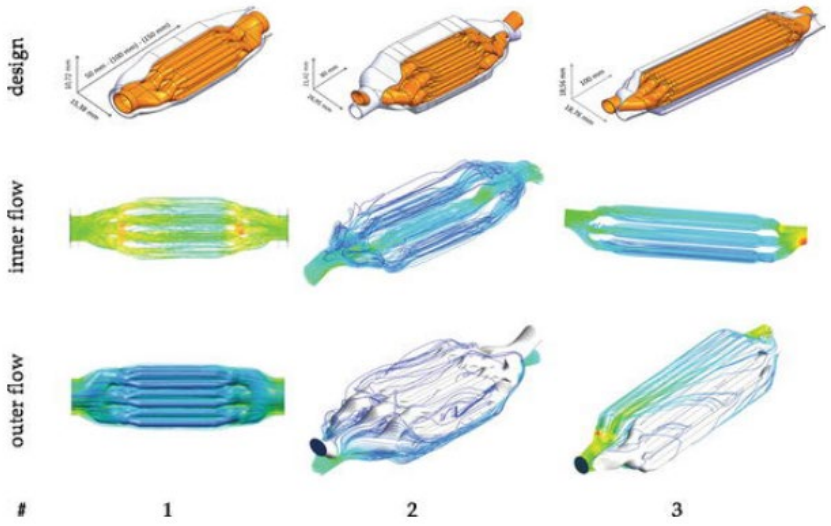

Figure 3.12 Shell-and-tube variation [18]

3.7.3 **Space filling curves**

An increased heat transferring area can make a HX more effective. To create corrugations of the curve that describes the inner wall, FASS-curves have been used [24]. They provide good control while using a simple definition. FASS stands for space-Filling, self-Avoiding, Simple, self-Similar. It is a class of curves that pass through every point of a grid without intersecting itself. When iterated they have a fractal behavior, shown with the Peano curve in Figure 3.13. Every line segment becomes similar to the whole curve in the next iteration.

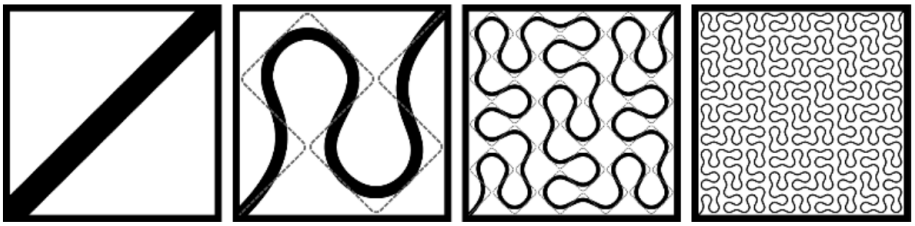

Figure 3.13 Four iterations of a FASS-curve, specifically the Peano curve [24]

The INSTAF project, a joint research project of research facilities and companies in Austria and Germany, have produced geometries suitable for HX or fluid mixing applications with this method [25]. Successively longer curves guide the dividing wall between two channels. Figure 3.14 shows one of the flows rendered to the left, and a manufactured prototype to the right. The results regarding performance are preliminary but promising.

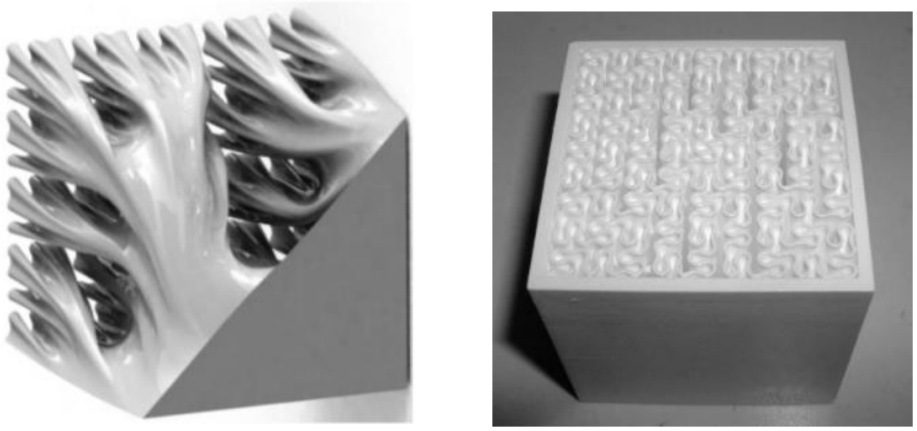

Figure 3.14 Peano curve loft [24]

3.7.4 **High temperatures**

In power generation the pursuit of better efficiency is leading to a higher operating temperature [19]. This makes the use of brazed HX impossible. Since AM HX are made from one monolithic material it is one way to solve this problem. The ambitious project HITEMMP launched 2019 aims to deliver an ultra-compact HX with the capability to work with 900°C and a pressure of 250 bar. Figure 3.15 shows a nickel super alloy prototype.

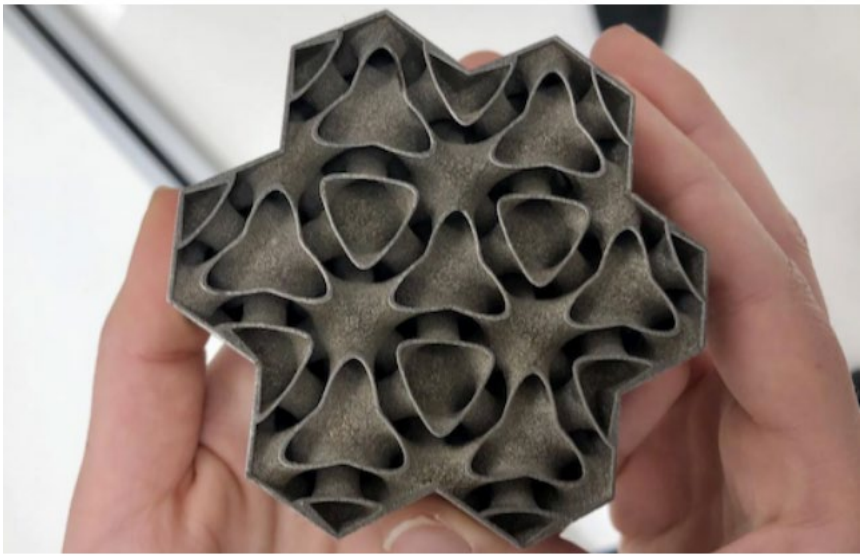

Figure 3.15 Nickel super alloy prototype [19]

Figure 3.16 shows a prototype HX for a micro gas turbine manufactured at Fraunhofer IFAM [18]. Some focus was put on designing for AM. The only post processing required were the machining of the inlet and outlet mating surfaces. The in- and outlets would not have been possible to manufacture without AM, but the internal structure resembles a conventional plate HX with wavy plates.

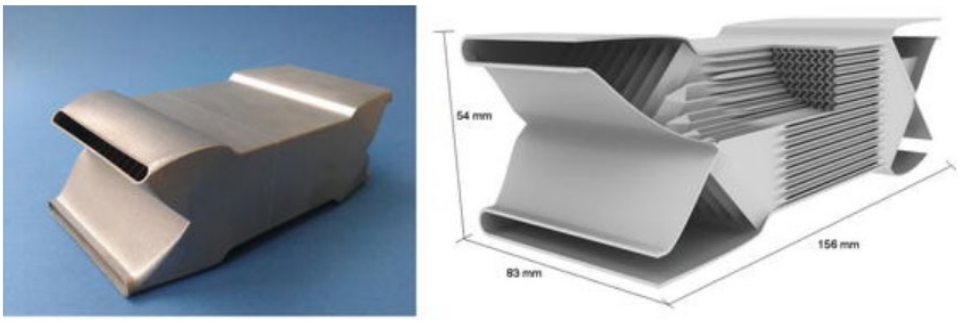

Figure 3.16 Prototype HX [18]

3.7.5 **Topology optimization**

Topology optimization has been used to find geometries with high heat transfer and low pressure drop. Work has been done on the situation of a heat sink and one fluid flow, but to the best of the authors' knowledge it has not been done with two fluid flows. One example is shown in Figure 3.17 [26] where a fixed proportion of the design space was assigned to a fluid flow (white), and the rest to a solid material of a constant temperature (black). This material distribution problem is a 2D simplification of reality.

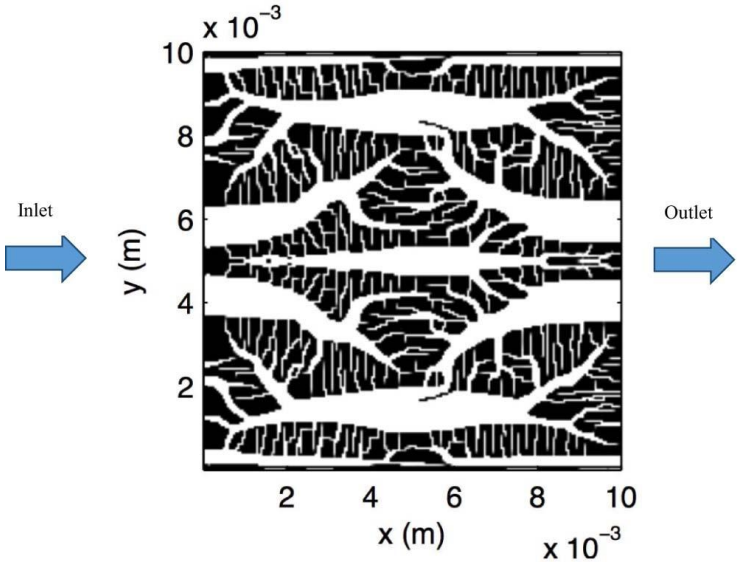

Figure 3.17 2D topology optimization [26]

Similar optimizations have been done in 3D [27]. Many inlet velocities were used, highlighting the difference between laminar and turbulent flow. Figure 3.18 shows a Reynolds number of 5000 to the left and 50 to the right. The resulting shapes have some similarities, but look very different. They also differ substantially from the results shown in Figure 3.17, accentuating the fact that boundary conditions and assumptions used must be closely examined before drawing general conclusions.

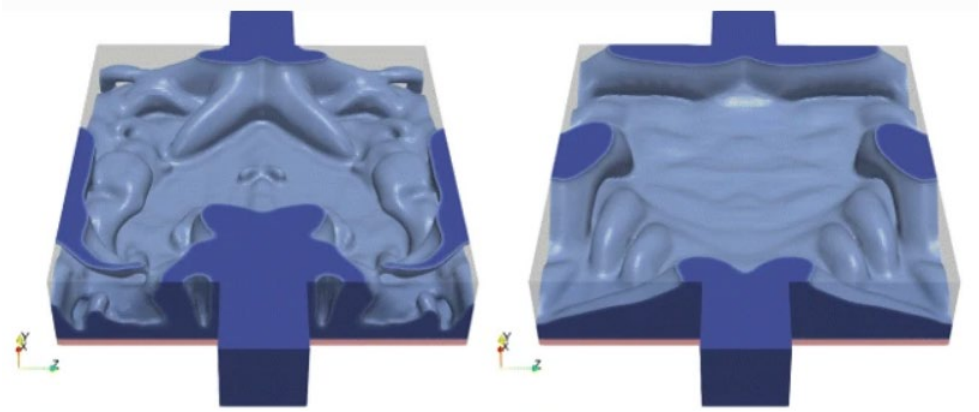

Figure 3.18 3D topology optimization [27]

Because AM can produce organic, irregular shapes without an added cost, it is well suited to use in combination with topology optimization, and can be the only way to realize such a concept.

3.7.6 **Extruded advanced cross sections**

Simple plate HX and shell-in-tube HX share the property of having the same cross section extruded along its whole length, with the two flows in alternating compartments. To use the same concept but with much more advanced channel cross sections have been proposed as a design path for AM [18]. The shapes can be optimized with CFD to provide a high heat transfer to pressure loss ratio. Examples are shown in Figure 3.19.

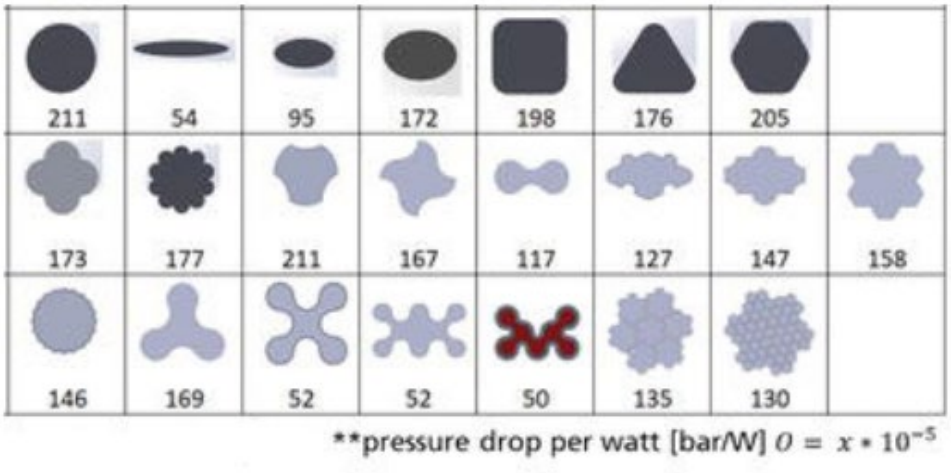

Figure 3.19 Pipe profiles [18]

The compartments can also be co-axial, because AM can produce the manifolds needed to supply such a structure. Cross sections can be twisted along its extrusion to increase internal mixing.

3.7.7 **Triply periodic minimal surface**

One promising concept for AM heat exchangers is to use a class of structures known as Triply Periodic Minimal Surface (TPMS) [28]. They are continuous surfaces that divide 3D space in two or more separated domains. Examples of the unit cell of different TPMS are shown in Figure 3.20. One of the domains are visualized as solid, the other as void.

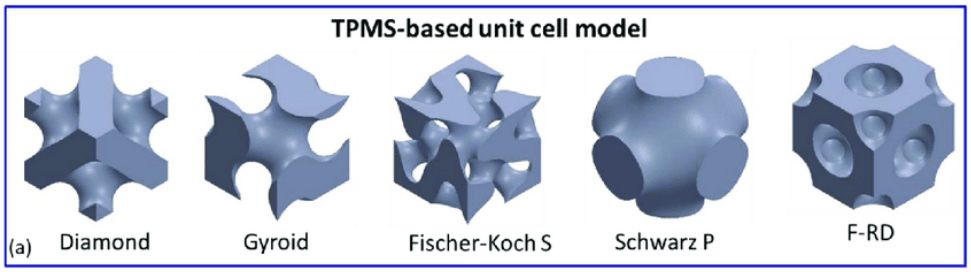

Figure 3.20 TPMS unit cells

When the unit cells are stacked in 3D-space two or more identical, intertwined 3D channel networks are formed. They resemble two interpenetrating crystal lattices that have been inflated until they meet each other. The two most studied variations are the Diamond and the Gyroid, shown in Figure 3.21 and Figure 3.22. They both have a cubic unit cell and two interpenetrating separated domains.

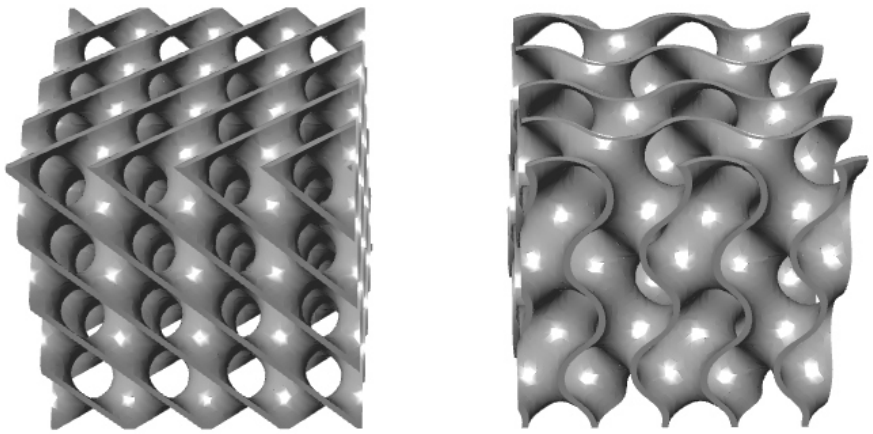

Figure 3.21 Diamond and Gyroid walls

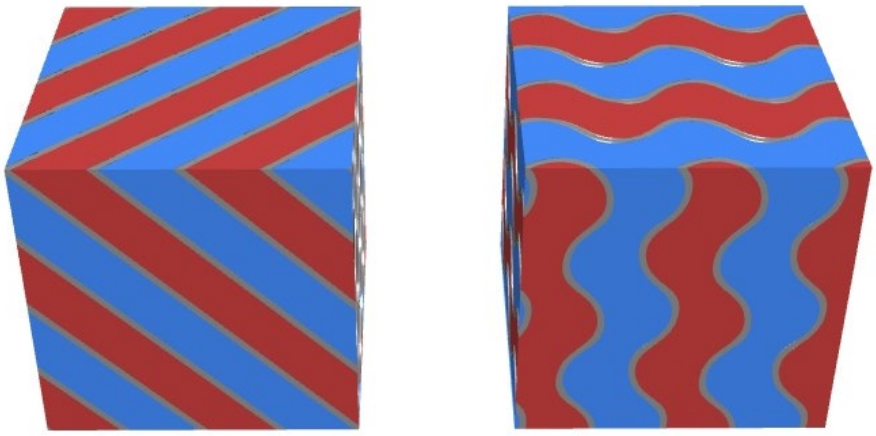

Figure 3.22 Diamond and Gyroid domains

Trigonometric equations can be used to describe the TPMS. Coefficients are used to translate and scale it along different axles, and to offset the boundary surface if different volumes are desired.

The large area to volume ratio, continuously connected surface, inherent structural integrity and potential for good mixing makes them a suitable avenue for HX applications. Proof-of-concept comparisons shows that the Diamond structure gives the highest heat transfer per unit surface and the lowest pressure drop per transferred watt of the compared TPMS varieties, shown in Figure 3.23 [29].

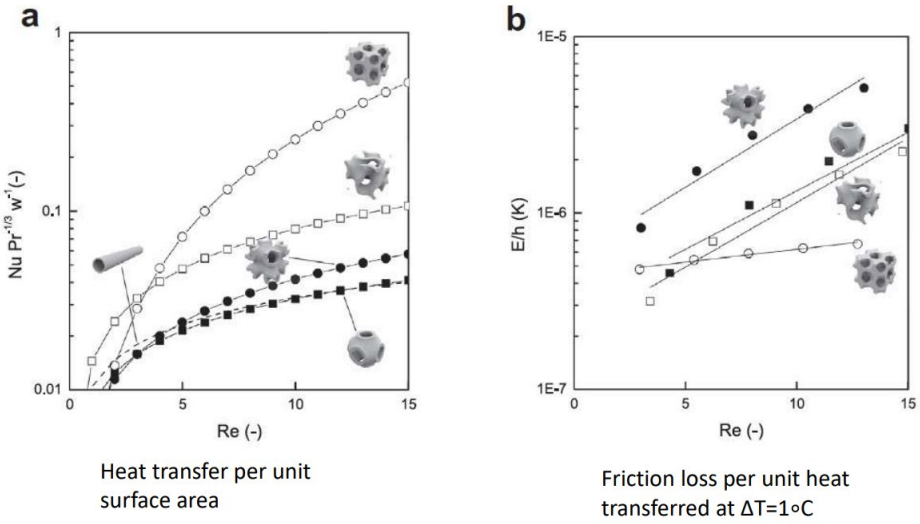

Figure 3.23 TPMS comparisons

A comprehensive work on designing a complete heat exchanger based on TPMS was done at the University of Notre Dame in 2019 [30]. The Gyroid, with a periodic length of 10mm, was chosen as the inner structure. This was motivated by its believed ability to resist fouling due to the spiral motion of the flows. A rectangular outer shape was chosen. CFD was performed to verify the design before printing on an EOS M290 EBM machine. The wall thickness used (0,2mm) was found to be insufficient, resulting in leaks between the channels. This prevented the part from being tested, but CFD was compared to a reference plate HX. This showed a 7,5 times increase in transferred heat in the TPMS HX compared to a reference plate HX, at an inlet of velocity 20mm/s. Pressure drop is reported to be 19 times higher. It should be noted that the CFD assumed a counter current configuration, something that was not realized for one of the flows in the model. As seen in Figure 3.24 one flow is oriented diagonally, flowing through the structure at an unexamined angle.

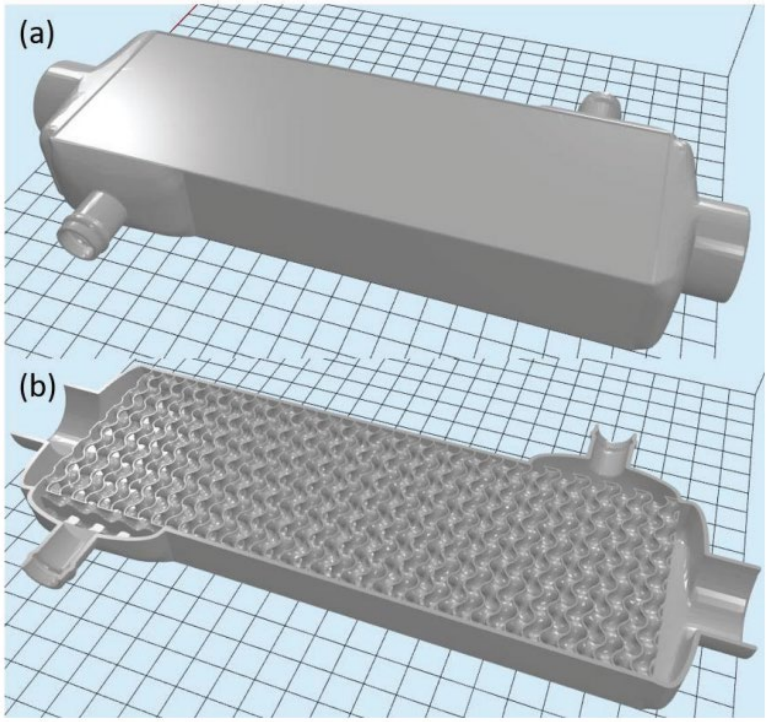

Figure 3.24 3D model of Gyroid HX [30]

TPMS have also been evaluated for mass transport through micro membranes [28]. Because of the analogy that exists between heat and mass transport, this was done by evaluating their ability for heat transfer. The study reported that the four manufactured TPMS samples outperformed the conventional hollow-tube variety by orders of magnitude. Of the tested samples, Schwarz-D (Diamond), was the one with the highest heat transfer in relation to its pressure drop. Figure 3.25 shows examples of the samples, manufactured with vat polymerization (resin printing in layman terms).

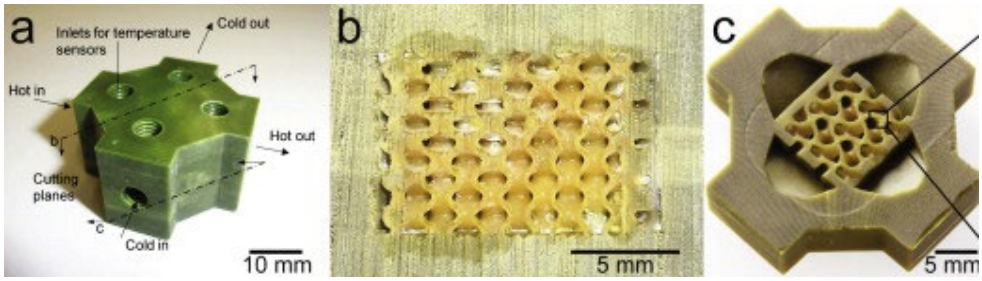

Figure 3.25 micro HX

4 Concept generation

In this chapter, theory and research is boiled down into concrete design guidelines for an AM HX. Then concepts generated with these in mind are presented.

In section 4.5 concepts are presented using their working names, given to concepts to help with quick communication in the project.

4.1 Designing for heat transfer

It is important to make efficient use of the material making up the HX, to reduce weight and reserve more of the total volume for the flows. If a fixed volume is to be distributed it should be put so that heat must travel the shortest path from one flow to the other. This means that the material preferably should be used for walls directly separating the two flows, and that the walls should be as thin as possible. This will increase heat transfer compared to if the heat must flow along the walls, or through thick sections. This means that fins are a less useful way of distributing the material.

This reasoning is demonstrated with a simple heat flux simulation in Autodesk Fusion 360. The part seen in Figure 4.1 represents a simplified version of a wall dividing two liquid flows of different temperatures. One flow is above the horizontal surface, the other below. Constant temperatures are applied to both sides: 60 °C on the upper sides and 10 °C on the lower sides. Flow patterns and temperature gradients caused by the transferred heat will of course affect the real-world situation, but the simulation gives an indication about the inherent nature of this principle: The material directly separating the two flows have higher heat flux (horizontal walls) than the fins being surrounded by a single flow (vertical walls).

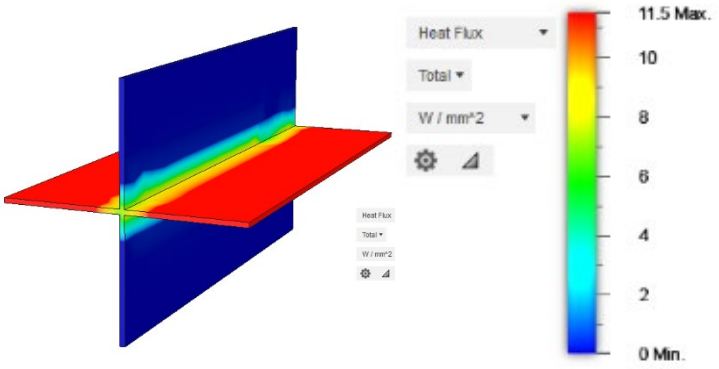

Figure 4.1 Heat flux demonstration

4.2 TPMS

Because the TPMS structures explored in Section 3.7.7 have good potential to fulfill the criteria described in Section 4.1 they were further investigated. Many TPMS varieties were explored, but the Gyroid and Diamond were of extra interest. The majority of the investigation was performed on 3D models in GH. Steel wire frame models, FFF printed models and sketches were also used.

Possible flow directions were investigated. The directions described with the vectors (1,1,1), (1,1,0) and (1,0,0) were compared. To reduce pressure drop a continuous cross section area of each flow is desired, as repeated reductions and expansions create pressure drop. The directions of the different channel segments are also interesting. Based on these considerations a flow along (1,0,0) was found to be the most suitable flow direction for both the Diamond and Gyroid. Figure 4.2 show a FFF printed form study.

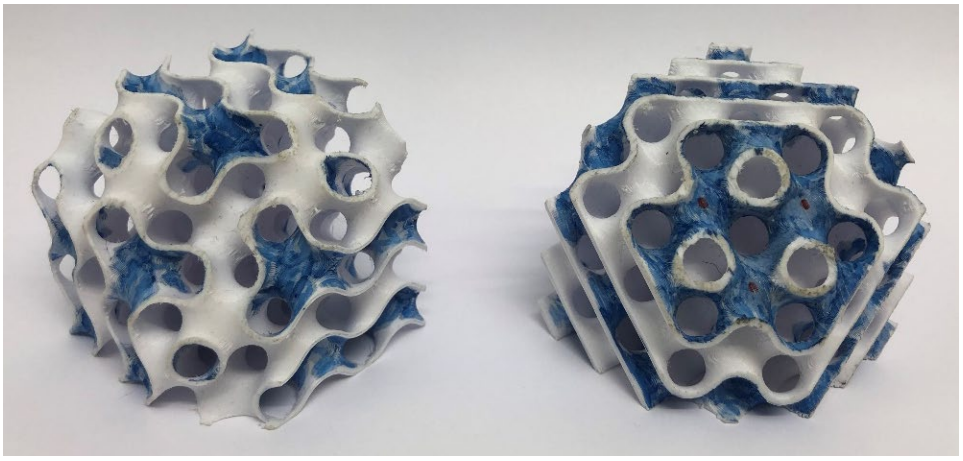

Figure 4.2 FFF printed models

As an intersection plane is moved through the Diamond structure along the chosen axis the cross section transitions back and forth between two principal varieties as shown in Figure 4.3: One square grid and one banded shape. The Gyroid provides similar intersections, but rotated 45° and with wavy lines.

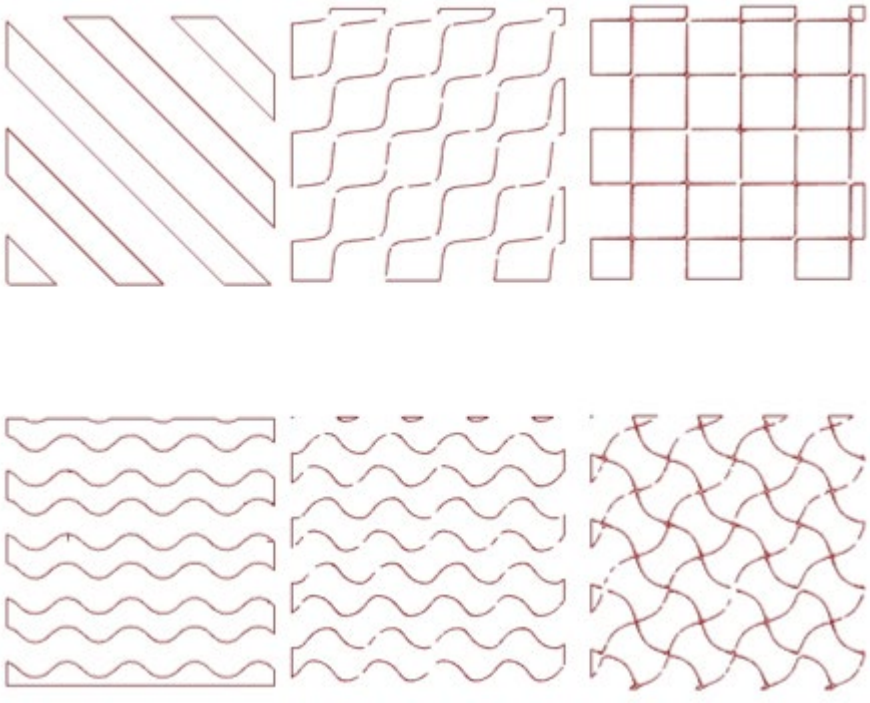

Figure 4.3 Diamond (top) and Gyroid (bottom) cross sections

4.3 Manifold

To allow counter current, the inlet of one flow should face the same section of the HX as the outlet of the other flow. A corresponding situation exists at the other end of the HX. The single channel of the inlet must divide in a way that supplies the internal structure of the HX that consists of multiple channels. The principle is illustrated in Figure 4.4, showing an example of cross sections where red symbolizes one flow (hot) and blue the other (cold). This seemingly simple problem becomes complex when considering that the two flows must be nested in the same volume, facing the same section.

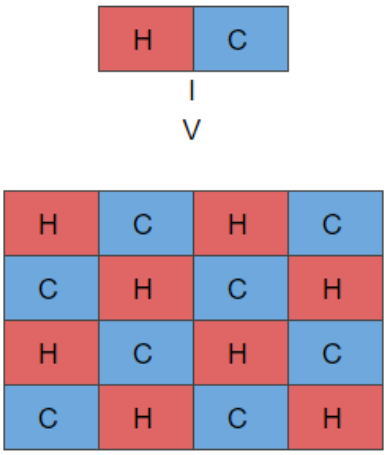

Figure 4.4 Manifold challenge. Red squares represent hot flows and blue squares represent cold flows.

4.4 Avenues to explore

Through research the following general observations were made:

- TPMS were found to be of extra interest.
- No examples of a true countercurrent TPMS HX were found. In- and outlet positions affect flow configuration. Position choices were seemingly made to make modeling easier, motivations suggesting otherwise were not found.
- The TPMS structure was handled similarly in all cases i.e. encapsulating it in a primitive shape e.g. boxes.

- Either manifolds or middle geometries were designed for AM (referring to complexity) but seldom both at the same time.
- The contribution to pressure-drop from the manifolds are often overlooked.
- A manifold design specifically suited for interfacing with TPMS was not found.
- It could not be concluded through research which is better suited for a HX: Diamond or Gyroid.

From the findings above, the aim of the concept generation was set:

> *Design a HX for AM by duly encapsulating a TPMS that interfaces with an appropriate manifold which provides full countercurrent flow. Make one Gyroid and one Diamond variation. Make one comparison sample with only the manifolds facing each other.*

The comparison sample is made as a way to indicate the influence of the inner structure versus the manifold, when it comes to pressure drop and heat transfer.

4.5 Manifold concepts

Concepts were developed around the manifold challenge.

4.5.1 **Tree**

One way to divide a flow is to have a tube branch like a tree. There are numerous ways to do the branching, see Figure 4.5 for examples. It can divide successively in many steps, or directly to all flows. If the layout is more elongated, a lower pressure drop can be expected. If the branches have a steeper branching angle the arrangement on the other hand occupies less space. If this shape is oriented in the build direction it is very favorable in terms of manufacturability. If the path through each channel has the same pressure drop, the distribution will be even.

Figure 4.5 Tree concept prototypes

This concept can be used as an inlet/outlet manifold for something similar to a shell-and-tube HX. It can also serve as an entire HX on its own, as shown in Figure 4.6.

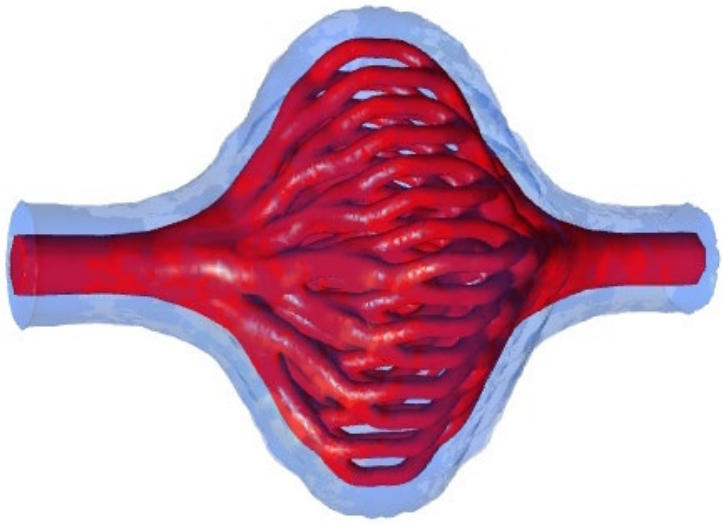

Figure 4.6 Double tree

As discussed in Section 3.7, the flow surrounding the tree often contributes with large pressure losses. Since diverging parts cause more problems than converging parts, an arrangement can be made where the inlet is always in the tree, and the outlet on the outside. This can be avoided if two trees can be made to nest into each other. No feasible way to do this was found.

4.5.2 **Decreasing grids**

The transition from a single inlet and outlet to multiple channels, as described in 4.2, can be translated to the transformation of a grid to a finer pitch of the same grid. If a way is found to do this, the design can be stacked. The last step of the grid can then be adapted to fit the channels. This is a general concept that can be used in

many counter current manifold applications. For two flows, nodes must have an equal number of connecting walls to avoid adjacent sides of the same fluid. A square grid or a triangle grid can be used, while a hexagonal cannot. To increase surface area, the walls connecting the nodes can be modified. Inspiration could be derived from M.C. Escher's extensive work on tiled space filling patterns, an example of which is seen in Figure 4.7 [31].

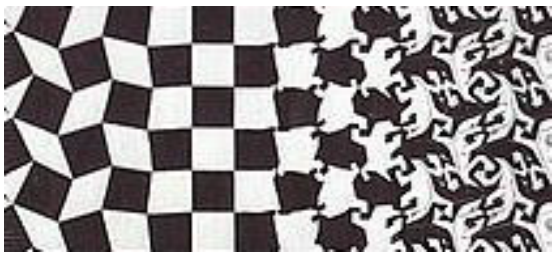

Figure 4.7 "Metamorphosis III" [31]

Sketches provided the first ideas. If the two small squares marked with red Figure 4.8 positions at all corresponding places this is achieved.

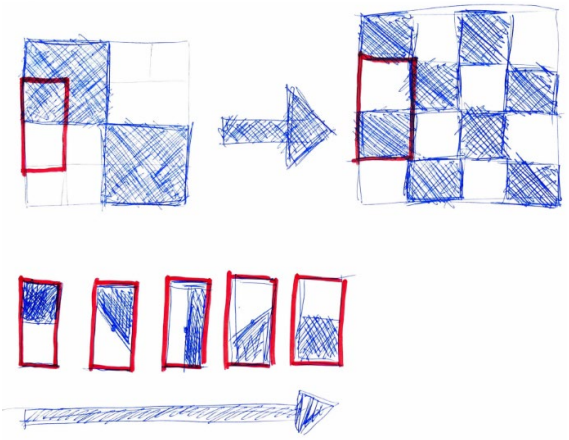

Figure 4.8 Decreasing grid sketch

CAD models were made to further visualize variations of the concept as shown in Figure 4.9

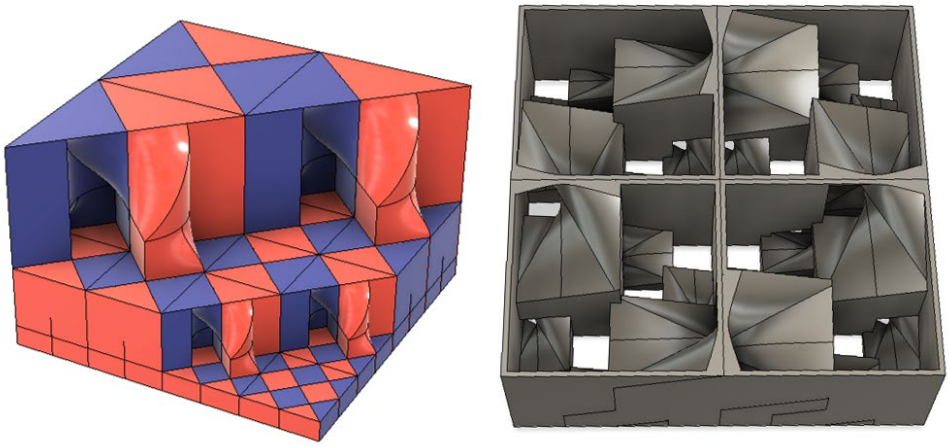

Figure 4.9 3D decreasing grid variations

A variation based on the triangular grid was also produced. Figure 4.10 show the top and bottom of the transition, as well as a perspective view.

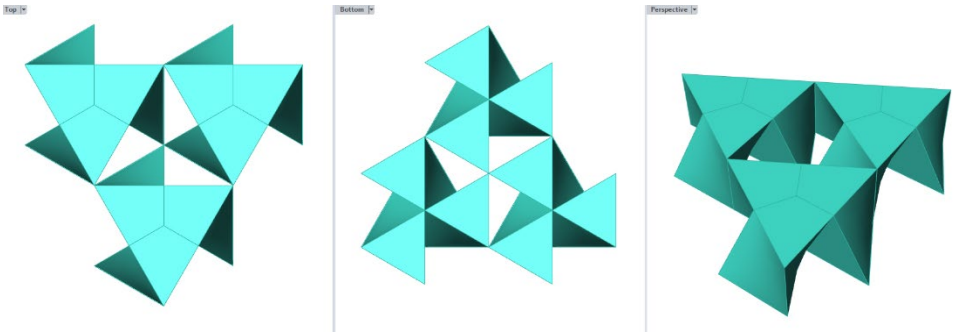

Figure 4.10 Decreasing triangular grid

This concept has potential, but no variation that was suitable for the application was found. It is therefore not found in the concepts selection, Chapter 5.

4.5.3 **Jolly Roger**

With a checker pattern cross section interface into which a fluid is to be distributed, the Jolly Roger manifold fuses every square of one flow. The morphing together of a flow happens gradually as distance from the checker pattern interface increases, see Figure 4.11. The final cross section shape is arbitrary. Inherent of this design is a flow distribution that is favoring the central part of the cross section. The squares of the other flow will also fuse and surround the first flow, which results in unsymmetrical flows.

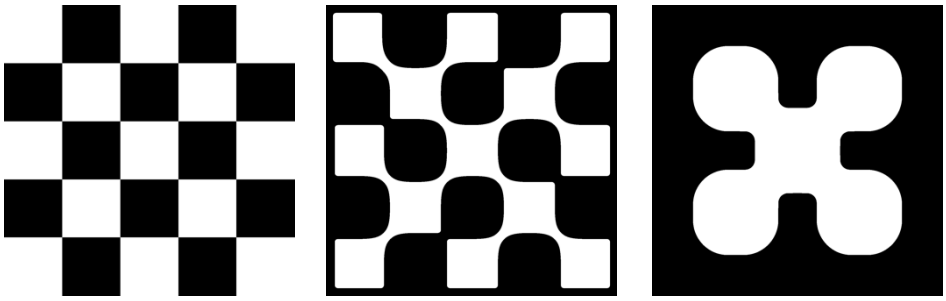

Figure 4.11 The transitions from a square grid cross section to an arbitrary cross section

A lofted version of this concept was modeled and is depicted in Figure 4.12.

Figure 4.12 The Jolly Roger concept in 3D

4.5.4 **Space filling curves**

The idea of using FASS-curves, (see Section 3.7.3) was further explored. Because they are self-similar, a smooth transition without collisions is possible between two successive iterations, making these curves interesting for flow distribution. Many curves were considered and the candidates with the most potential were modelled in GH using L-systems generated by the plugin "Rabbit" [32]. An L-system, or Lindenmayer system, is a parallel rewriting system first described in the influential book The Algorithmic Beauty of Plants [33]. It can create complicated patterns with only a few simple rules, like the plants depicted in Figure 4.13.

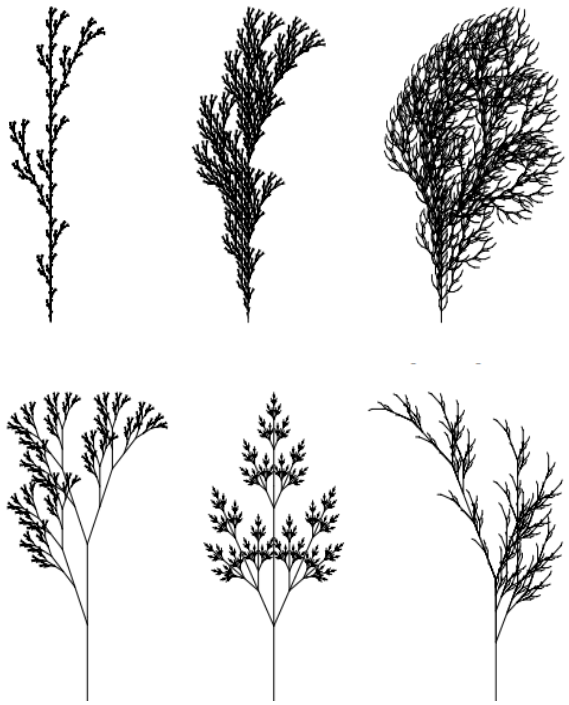

Figure 4.13 L system plants [33, p. 25]

Every L-system definition consists of an alphabet of operations, a starting axiom and production rules that are iterated. The Peano curve geometry found during the research phase was re-modelled in GH. This FASS curve has the benefit of forming a checker pattern if the radiuses are removed, allowing direct access to the Gyroid or Diamond structure if the square grid section is used. The cross sections were scaled, to modify the shape from a mixing device to a manifold. Figure 4.14 shows one flow in red and one flow in transparent blue.

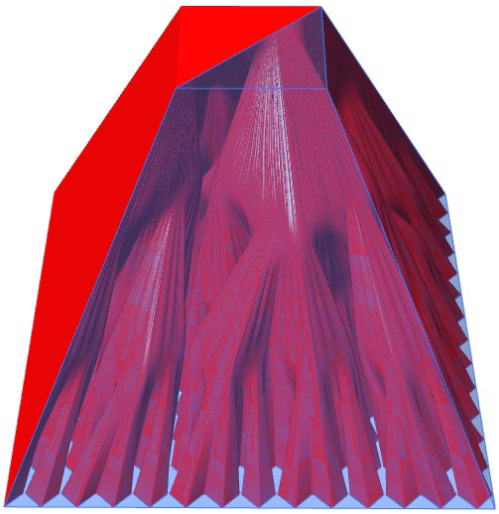

Figure 4.14 Tapered Peano loft

Another, novel, variety was modelled using the "Square" curve [34]. It is created by the following L-system:

Axiom: X

Production rule: X=XF-F+F-XF+F+XF-F+F-X

In this alphabet "X" is a placeholder variable to be iterated and "F" draws a line in the current direction. A 90° left turn is written with "-", a right turn with "+". Its four first iterations are represented in Figure 4.15 (pictures from GH). The curve creates the outline of the black areas, which represent one flow. The white area represents the other flow. The definition stated above creates half of the shape, which is then mirrored over the diagonal. A fillet is introduced after the curves are constructed.

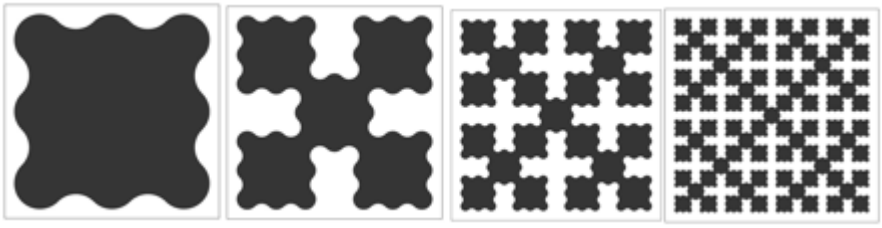

Figure 4.15 Square curves

Guide rails were created to connect the curves, and a net surface was constructed. When the different sections are differently scaled it creates a transition from two coaxial pipes to a distributed pattern. One flow is represented with red in Figure 4.16, the other in transparent blue. An important consideration with this geometry

is that it does not produce either of the sections available in the TPMS. Some transition geometry therefore has to be constructed.

Figure 4.16 Square curve loft

These concepts are mainly considered for use as manifolds, but they could also be used as a complete HX if one inlet- and one outlet version are combined. One important consideration is that the whole geometry consists of a single wall. This is not a problem if the part is short and connects to a rigid structure in both ends, but can pose a problem if a longer structure is created. The structural integrity must then be guaranteed, for example by adding connections between walls at some points.

4.5.5 **TPMS**

It was investigated if the TPMS structure in itself could make up the manifold. It can be trimmed and sealed off in a cone or pyramid shape. One example of how this could look was modeled and is shown in Figure 4.17.

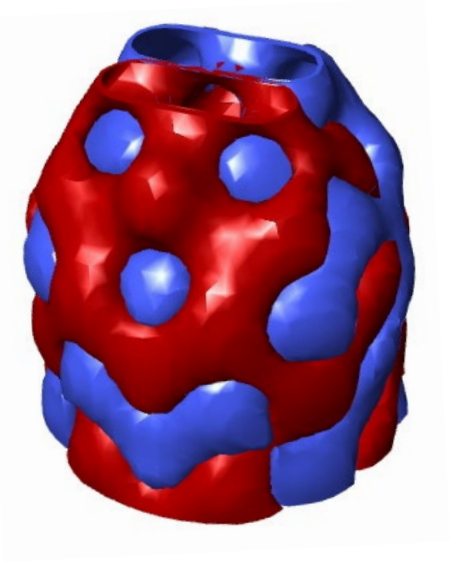

Figure 4.17 Trimmed TPMS

The two flows can be perfectly nested side by side within each other. Because the channels merge after each branching, more of the flow will be directed to the middle of the structure. This could be countered with pulling the walls inwards, creating smaller channels closer to the middle, but this poses a serious modelling challenge. A similar trimming of the Gyroid is harder, due to the more complicated and unsymmetrical nature of the channels.

4.5.6 **Clasping hands**

The Gyroid and Diamond TPMS have a banded pattern in one intersection. The simplest way we found to interface this pattern with an inlet, while still keeping all channels nested in one shape, is the concept called “Clasping hands”, shown as clay models in Figure 4.18.

Figure 4.18 Clasping hands prototypes

3D Voronoi cells were evaluated as a way to form this manifold, the seeds based on the rough paths from the bands to the desired output, see Figure 4.19.

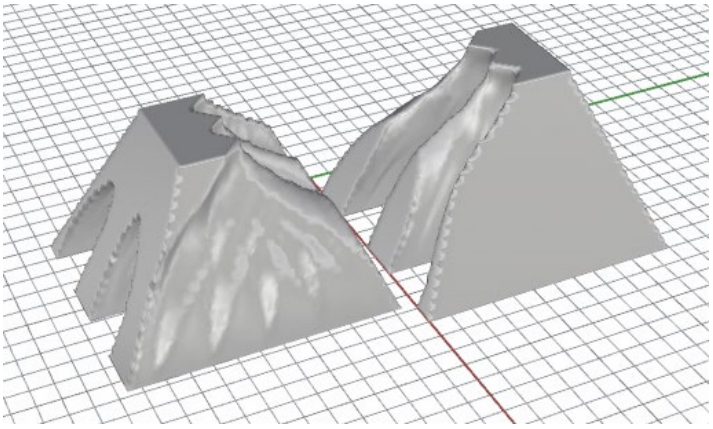

Figure 4.19 Voronoi clasping hands

A version with constant cross sectional area was modelled. The inlet and outlet have the character of two reservoirs, as seen in Figure 4.20.

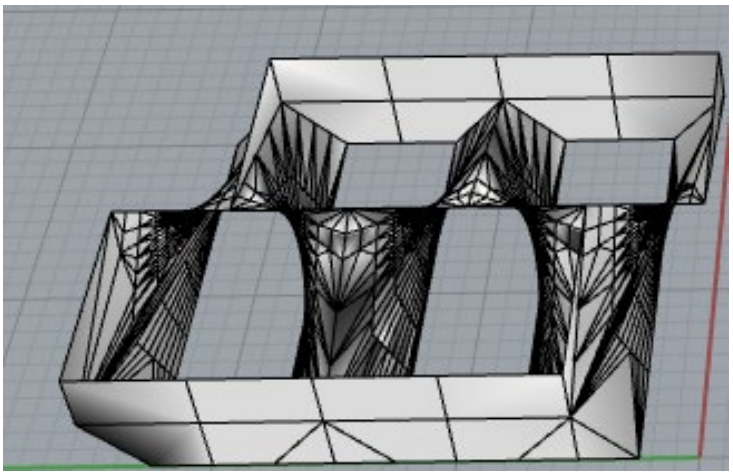

Figure 4.20 Clasping hands 3D model

If another level of this structure is applied below the first it provides a checker pattern interface with alternating flows, see Figure 4.21. This has great potential to interface with existing heat exchangers. One can imagine a conventionally manufactured plate-fin HX seen in Figure 3.4, where an AM manifold is added to enable counter current flow. But for the TPMS, only the top part is needed.

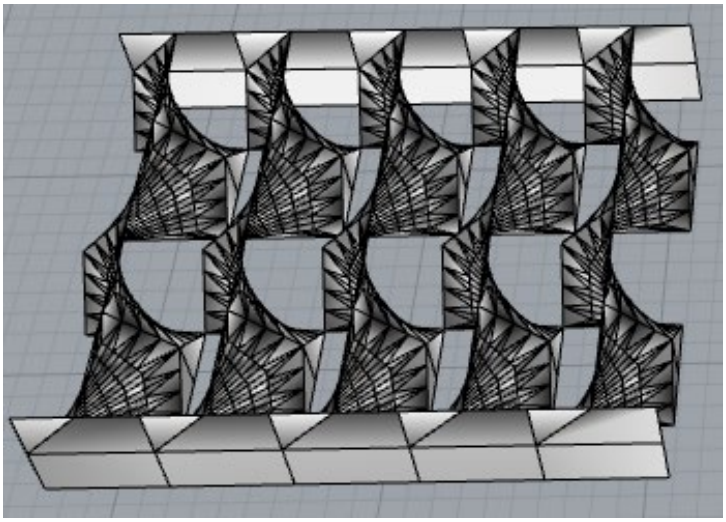

Figure 4.21 Clasping hands, additional level

5 Concept selection

A concept scoring matrix was used to rank the different manifold concepts and choose the most suitable concept to proceed with.

5.1 Selection criteria

The following criteria were used. Some criteria were discarded due to previously mentioned delimitations and circumstances, discussed in Section 1.3.

5.1.1 **Ease of modeling**

For an additively manufactured concept, the modelling becomes central to the resulting part. To easily reach the point of a finished 3D model that is true to the concept was deemed important to the success of this project and the usefulness of our results for replication. Each concept was ranked by estimation based on experience of modelling in GH and Fusion 360.

5.1.2 **Size**

As described in the objective of this thesis, size is one factor that will increase the efficiency of a HX. A smaller HX will save space and weight. Thus the manifold needs to be contributing to the size reduction if possible. Comparisons were made by decreasing the length of the manifold and discussing the effect that would have on its function.

5.1.3 **Support structure**

The support structure of a print needs to be removed in the post processing. If there are unreachable support structures in a printed manifold, its function is compromised and therefore not a suitable candidate to move forward with. External supports also add effort in the post processing. Concepts were compared with the

guidelines presented in Direct Metal Printing Design Guide to determine if they were at risk of needing unwanted support structures.

5.1.4 **Flow distribution**

For the HX to perform well, the fluids must enter the inner structure in a distributed fashion. Each concept was evaluated with hand waving arguments as to whether the fluid is distributed into all parts of the TPMS structure.

5.1.5 **Flow equality**

It is important that both the hot and the cold side have good flow characteristics, and that the design does not favor one of them at the expense of the other.

5.1.6 **Cross section adaptability**

Whether the manifold is useful for interfacing with cross sections or applications that are different from the scope of this thesis. It was judged on the basis of how the core concept would handle different channel configurations, according to our experience from prototypes of the concepts.

5.1.7 **Flexible channel count**

For further development it is valuable that the channel count can be varied without limitations, to provide greater design freedom. Scoring was based on experience from modelling concepts.

5.2 Concept scoring

Use of this method is discussed further in section 10.1.

Manifold concepts were compared according to the concept scoring matrix shown in Table 5.1. The concepts were ranked against each other, and when two were found to be equal an average score was given to both. The average score for each concept was used to compare them.

Table 5.1 Concept scoring matrix

	Ease of modelling	Size	Support structure	Flow distribution	Flow equality	Cross section adaptability	Flexible channel count	Average
Tree	4,00	3,00	3,00	5,00	1,00	5,00	2,50	3,4
Space filling curve	3,00	3,00	1,50	2,50	3,00	1,50	1,00	2,2
Jolly Roger	2,00	3,00	1,50	2,50	2,00	1,50	2,50	2,1
No manifold adjusted TPMS	1,00	1,00	5,00	1,00	4,50	3,50	4,00	2,9
Clasping hands	5	5	4	4	4,5	3,5	5	4,4

5.3 Decided concept

It was decided to use the “Clasping hands” manifold on both sides of all samples being made. Samples will have identical channel count, and identical wall thickness. One Gyroid and one Diamond sample will be created, both with a 50 x 50 x 50 mm middle part. A comparison sample will also be made, with only two manifolds facing each other, without a TPMS structure in the middle.

6 Concept realization

In this chapter, the principles and methods of modelling a countercurrent, encapsulated TPMS HX are shown.

6.1 Refinement

The concept was further specified before modelling. The Diamond and Gyroid variation went through the same following steps, but were treated separately.

A manifold-manifold without the middle TPMS structure was also modelled and printed, to use during experiments. The temperature difference and pressure drop measured on this part will give an indication of the influence on pressure drop and temperature difference of the manifold versus the TPMS part. This manifold-manifold part will be referred to as “Comparison” in this thesis.

6.1.1 **Wall thickness**

It was decided to use 0.5 mm as wall thickness in all parts, see Section 3.6.2. This is slightly above the recommended minimum thickness to produce reliable walls without voids [8]. Thicker walls decrease heat transfer.

6.1.2 **Outer walls**

To reduce dead zones in the TPMS, the structure needs to be cropped and enclosed in a way that respects the internal channels. A cut that allows the two flows to interact as closely as possible all the way to the outer boundary increases heat transfer. The skeletal model, which describes the center of the channels, is a useful tool to visualize the interaction of the two flows. This is shown in Figure 6.1.

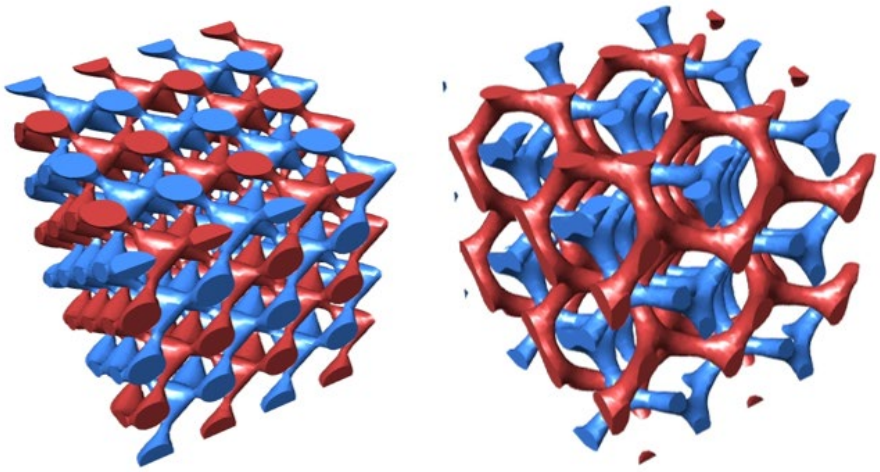

Figure 6.1 Diamond and Gyroid skeletal models

6.1.3 **Channel count**

A channel width of around 6 mm is desired. This is comparable to the ones found in the literature and is a good balance between the lower limit, (a too large portion of the volume is occupied by walls), and being too large (impossible to print because of the internal overhang). A 50 x 50 mm cross section, 8 bands and 0.5 mm wall thickness gives a channel width of 6.2mm. It was decided to use 8 bands.

Due to the different nature of the Gyroid and Diamond structure, the enclosing resulted in a different layout of the bands in the connecting section. 8 bands are therefore translated to 7 full bands and 2 half bands in the Diamond variation.

6.1.4 **Manifold**

A longer manifold was thought to give a more even and smoother flow, but a small size is also desired. It was decided to have the outer dimensions of a pyramid with sides sloping 45°. The in- and outlet were decided to enter normal to the pyramid's surfaces. This is thought to counteract the fact that the distribution of each flow's cross section area favors the side closer to the connecting pipe. ½" pipe threads should be used, because of the test rig available to the project. To avoid overhangs on the individual threads, the threaded connectors should be planed off at the top and bottom facing sides.

Two manifold variations have to be modelled, to account for the different intersection patterns of the Gyroid and Diamond.

6.2 Modeling

The same approach was used to create both the Gyroid and the Diamond HX. The approximate trigonometric definition for the respective TPMS were used:

$$\text{yroid} : (sin(x+dx)cos(y+dy) + sin(y+dy)cos(z+dz) + sin(z+dz)cos(x+dx)) * L = 0$$

$$\text{Diamond: } (sin(x+dx)sin(y+dy)sin(z+dz) + sin(x+dx)cos(y+dy)cos(z+dz) + cos(x+dx)sin(y+dy)cos(z+dz) + cos(x+dx)cos(y+dy)sin(z+dz)) * L = 0$$

The definitions were used as geometric sources in the GH plugin Monolith, through the *Function* block. The parameters dx, dy, dz and L were used to translate and scale the functions. Bounding surfaces for the outer walls were created, and defined as a Monolith geometric source. The Diamond structure only required a filleted box for its wall, while the Gyroid required a shape more adapted after its channels. A voxel volume was created with the Monolith plugin. The TPMS and the bounding wall each contribute with a density field in this volume. Examples of the contribution of each geometry is depicted in a slice plane in Figure 6.2.

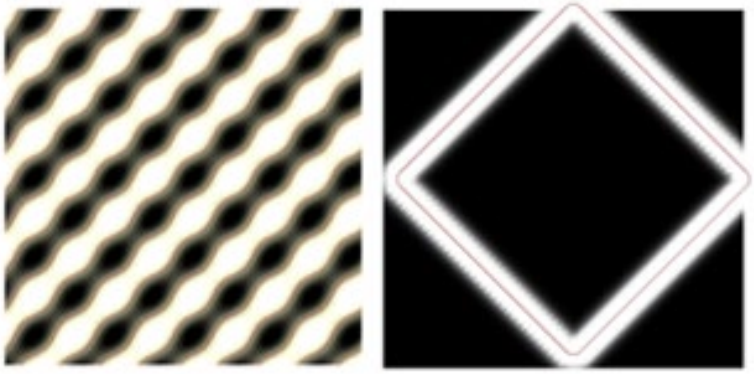

Figure 6.2 Density fields

The two density fields are combined, and their gradients are blended. Every voxel, similar to a 3D pixel, gets a value depending on its proximity to the two objects. This procedure is repeated, but with a negative geometric source for the bounding wall. Figure 6.3 shows the two resulting fields, each closing of one flow.

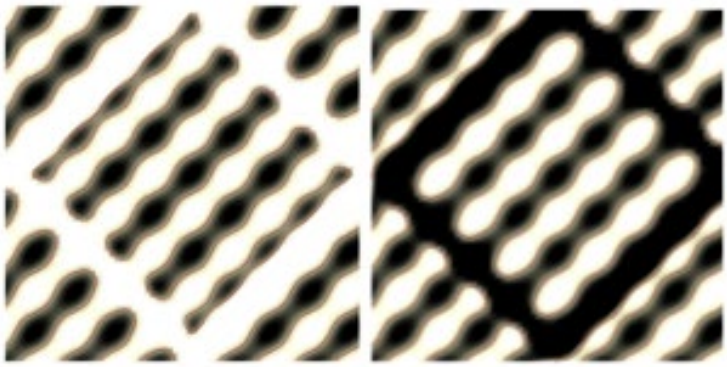

Figure 6.3 Resulting fields

An ISO surface can be extracted from the fields, providing a mesh tracing a certain value. For ISO = 0 the result is that the two flows are closed off, respectively. The walls have a smooth transition and can be adjusted to a desired bulging with the *Decay* and *Strength* parameters in the geometric source of the bounding wall. One of the closed flows, and the geometric source used to create it, is shown in Figure 6.4. The two resulting ISO meshes are combined further on in the process.

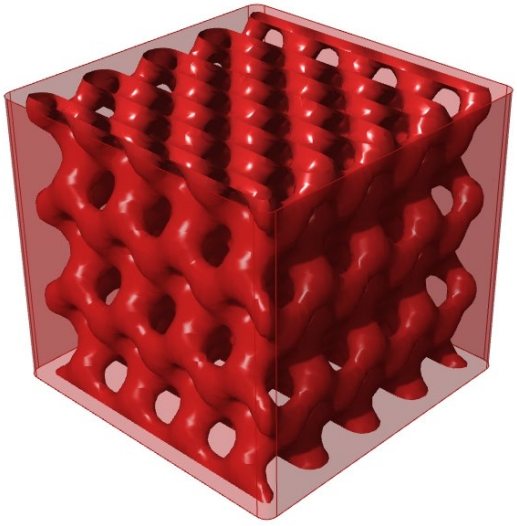

Figure 6.4 Bulbous TPMS

The manifold was constructed with the outer shape of a rectangular box and the internal structure created from a repetition of alternating surfaces. This is shown in Figure 6.5.

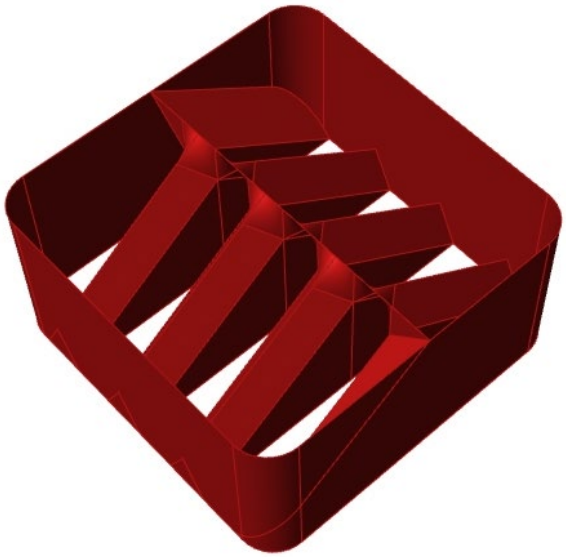

Figure 6.5 Un-tapered manifold

The combination of these elements was tapered to the shape of a pyramid and converted from a BRep to a mesh. The internal structure after the tapering is shown in Figure 6.6.

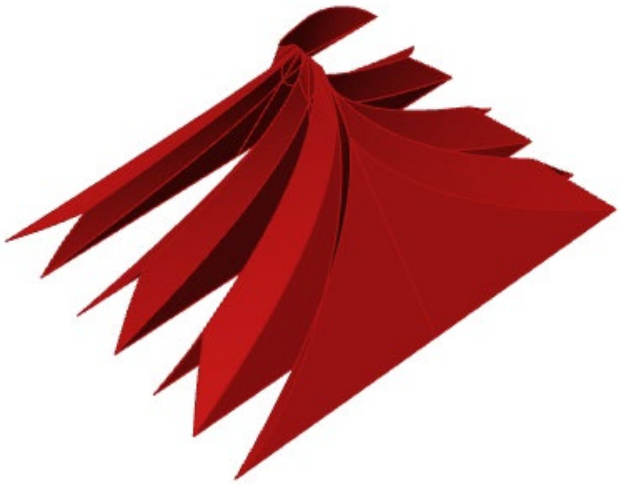

Figure 6.6 Tapered internal structure

The threaded connectors were modelled in Fusion 360, as it has better support for threads than GH. They were internalized as meshes in the main model. The complete manifold is depicted in Figure 6.7.

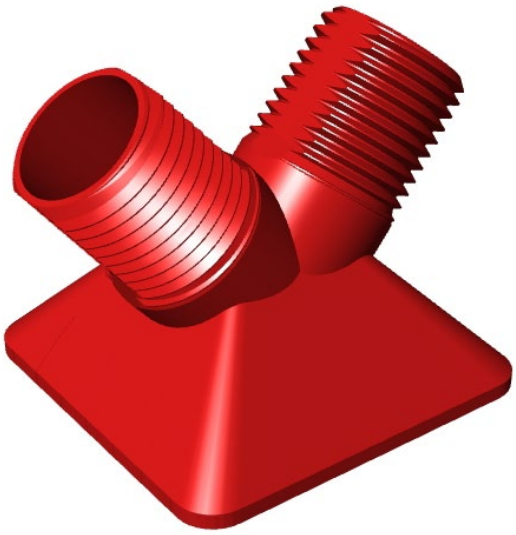

Figure 6.7 Final manifold design

The manifold is duplicated and positioned at both ends of the respective TPMS structure, with a 2 mm gap between the parts. Meshes were constructed to stitch the walls of the parts together. This is because the Gyroid structure has complicated curves describing the channels at its connection section.

The complete geometry is now described with mesh surfaces: The two overlapping TPMS channels, the two manifolds and the connection parts. There are no standard tool in GH to go from here to a 0.5 mm thickened watertight mesh. The Dendro volumetric modelling plugin was therefore used. All the mesh parts were converted to voxel volumes, in a similar fashion to the process of creating the TPMS walls. All volumes except the threaded connectors were then offset to provide the right wall thickness. The volumes were united, and a final mesh extracted for each sample. The script producing the Gyroid variety is presented in Figure 6.8, showing a summary of the described steps.

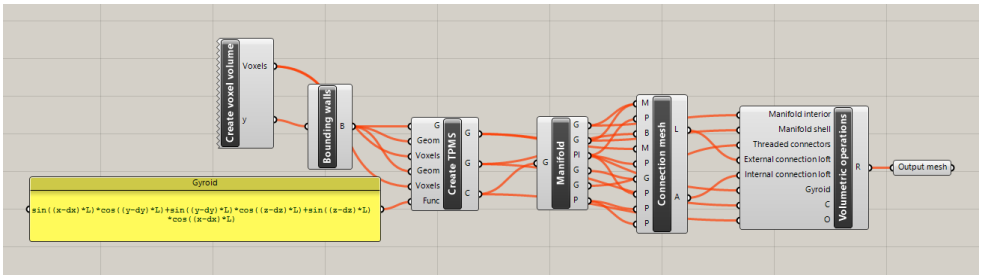

Figure 6.8 GH block diagram (summarized)

The different parts described in this chapter were combined into the three samples decided upon in Section 4.4. Figure 6.9 shows, from left to right: The Diamond variation, the Gyroid variation and the comparison sample.

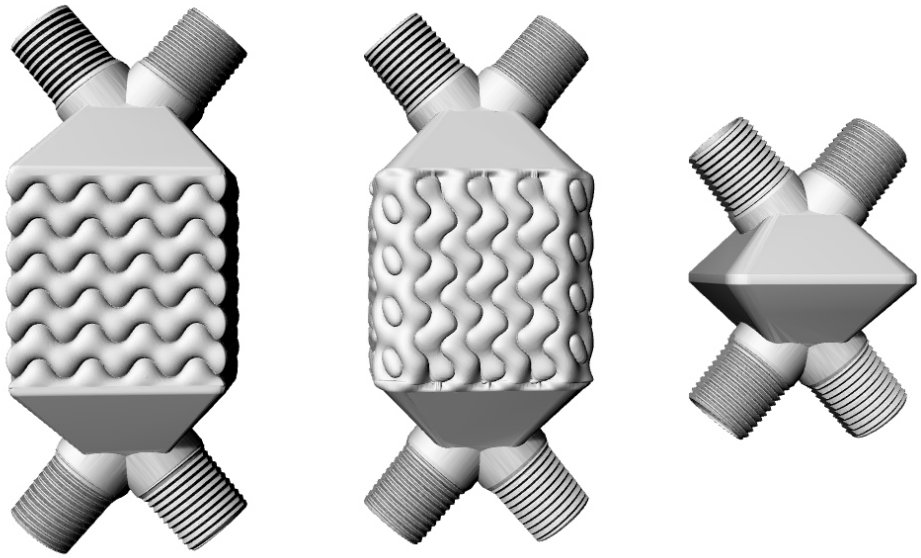

Figure 6.9 Modelled samples

7 Manufacturing

The three samples that have been modelled (Gyroid, Diamond and Comparison) were manufactured in with SLM in the aluminum alloy AlSi10Mg, supports were removed and heat treatment were performed. Some corrections were necessary before proceeding to testing.

7.1 Preparation

The three samples described in Chapter 6 were individually prepared for printing. The procedure was the same for all samples. First, the face count of the meshes were reduced in the program *Magics* to provide a faster slicing process. They were then oriented in the planned print direction in the program *3DXpert* and rotated 30° around the z-axis to reduce the risk of the scraper to get caught at the straight edges. A 1.0035 scaling factor in X and Y direction was introduced by the software to compensate for shrinking.

The parts were raised 5 mm off the build plate. Supports were added to the rim of the lower threaded connectors as seen in Figure 7.1. Since this area is easy to access for post processing, solid supports were used.

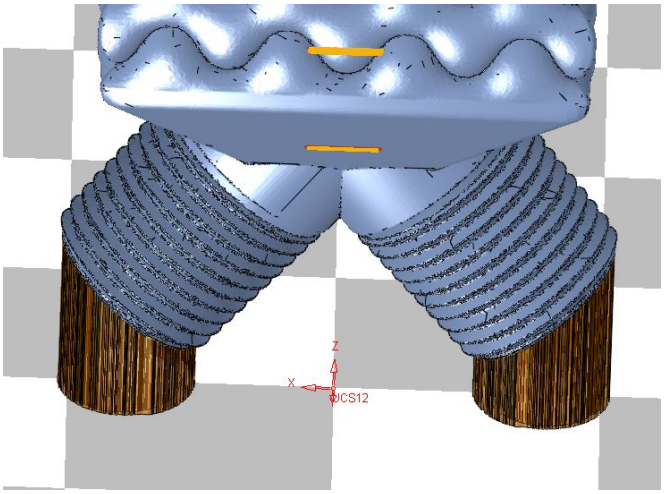

Figure 7.1 Supports

Because all parts have identical geometric features facing the build plate the supports were identical on all three. The internal channels have a diameter below what is stated as the threshold for internal circular channels and were not given support. This is expected to result in a coarser surface finish at those places, which was considered acceptable. The parts of the threads exceeding the overhang limit were so small that they were not given support.

The models were sliced individually. The layers were inspected to ensure no gaps or other imperfections were present. The software *DMP Control* was used to position the sliced parts relative to each other in the build chamber. Seven other objects were printed in the same run. The parts were placed in a way that accounted for the movement of the scraper, the risk of small parts getting dragged along by it and the gas flow.

7.2 Printing

Printing was observed occasionally through the observation window of the machine, as seen in Figure 7.2. The scraper is seen to the right. Some parts were observed to rise above the build layer due to warping. The scraper was however not damaged by this. The print results were satisfactory, see Figure 7.3.

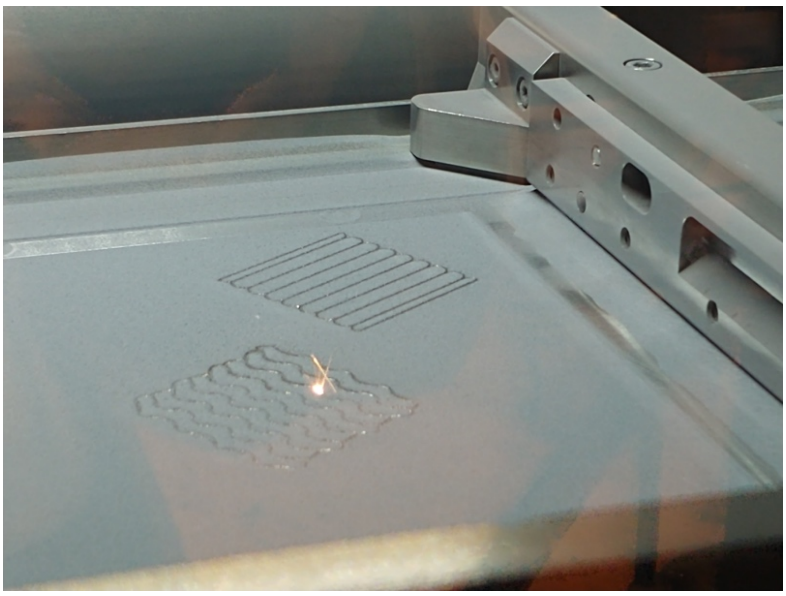

Figure 7.2 Laser scanning

Figure 7.3 Part excavation

7.3 Optical inspection

Surfaces with different angles against the print direction had different surface roughness, as expected [8]. Surfaces that were built facing down had characteristically coarse surfaces while those built facing up were smoother. Figure 7.4 shows a 45° upwards facing surface to the left, and a 45° downwards facing surface to the right.

Figure 7.4 Direction dependent surfaces

It was found that two threads on each sample were reversed, effectively making them left handed. A noticeable hole was found in two of the corners of the Gyroid sample.

7.4 Post-processing

7.4.1 **Powder Removal**

While still attached to the solid aluminium build plate, holes were drilled in the supports to access powder stuck inside the parts. Vacuum cleaning and turning the build plate in different orientations were used to remove loose powder.

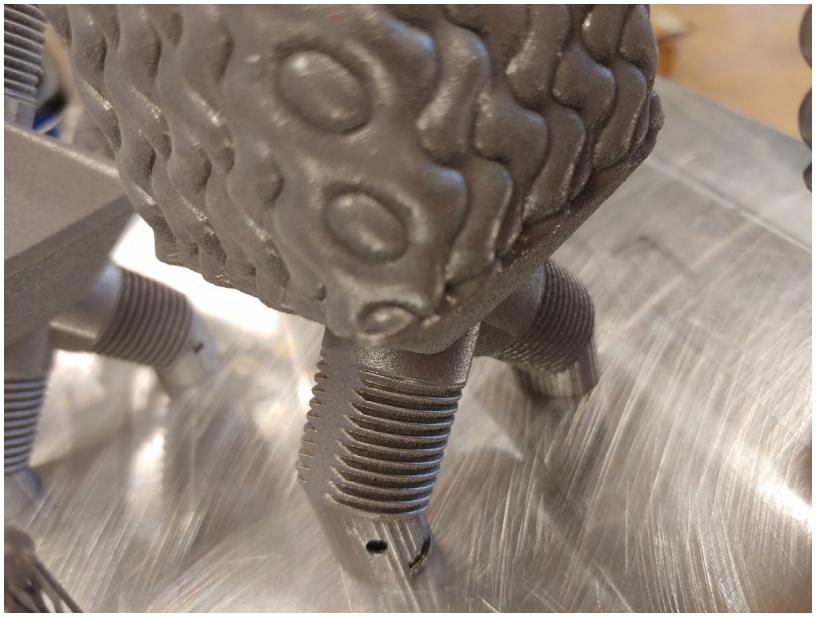

Figure 7.5 Drill holes

7.4.2 Build Plate Separation

The parts were band-sawed off the plate (see Figure 7.6). The decision to separate the parts from the build plate before thermal treatment was based on the following factors:

- The mass of the plate is big compared to the parts, making heating slow and uneven.
- The parts are not likely to warp beyond acceptable levels because of their geometry.
- The build plate does not fit in the available furnace.

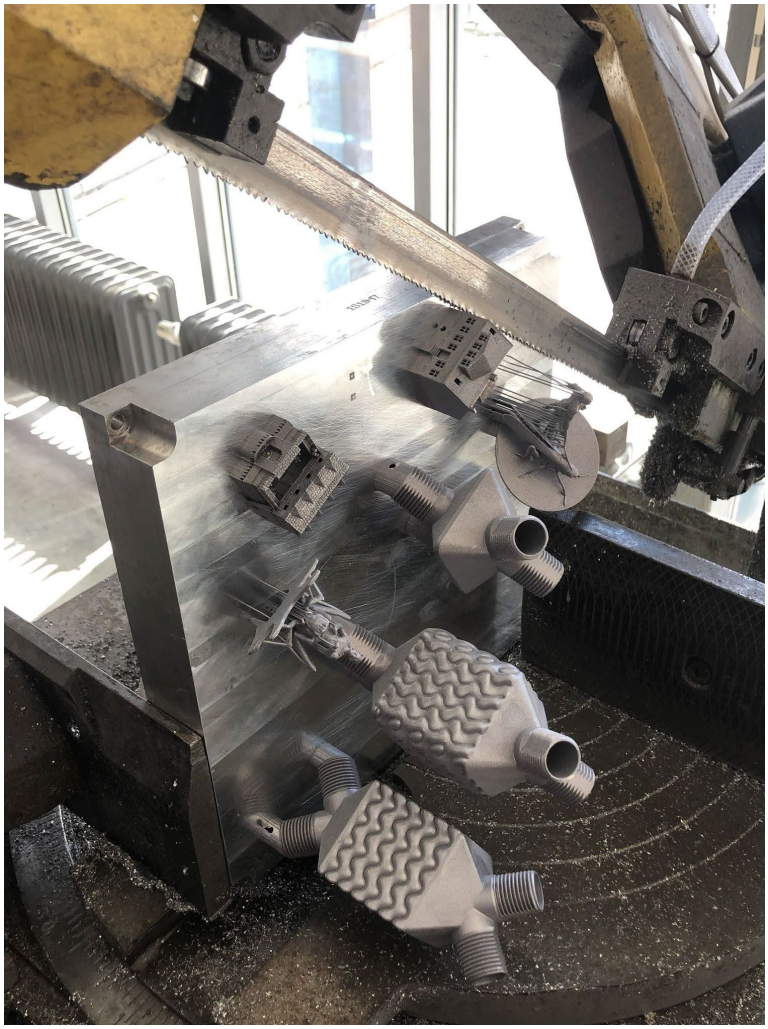

Figure 7.6 Build plate separation

7.4.3 **Thermal Treatment**

The parts were heat treated with a 30 min temperature ramp up to 300 °C and held for 1h30m. Access to a furnace was provided by the Faculty of Materials Engineering at LTH. The layer of oxidation on the parts appeared to have increased due to the unprotected atmosphere during heat treatment but were still within acceptable levels. Figure 7.7 shows how the parts were positioned in the middle of the furnace, to provide a uniform heating.

Figure 7.7 Heat treatment

7.4.4 **Support removal**

Anomalies were found in two of the support structures, see Figure 7.8. It is not known where they have originated from. Supports were grinded away, and the mating surfaces for the washers were filed flat.

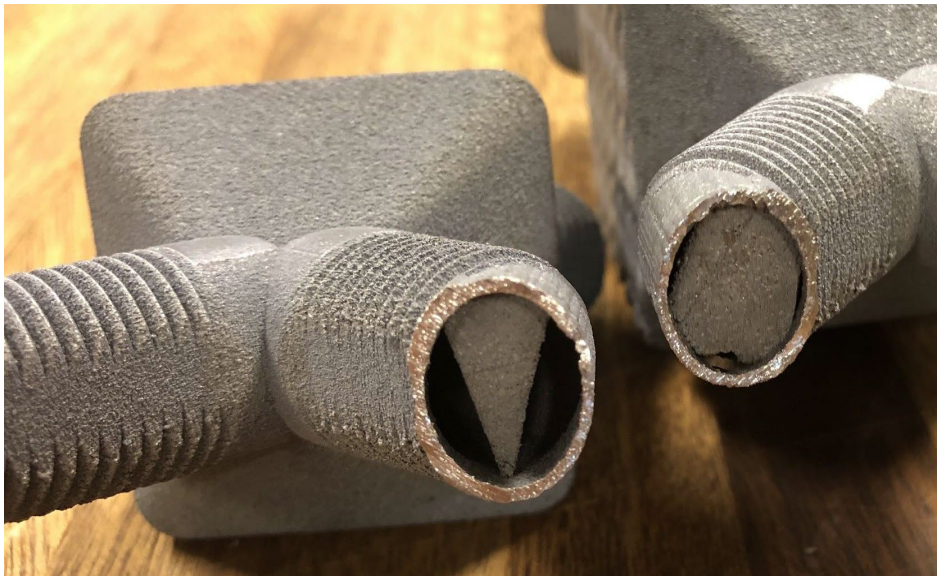

Figure 7.8 Unexpected structures in supports

7.4.5 Corrections

The incorrect threads were re-tapped, losing some definition but gaining full functionality. Figure 7.9 shows the process. The correct threads were also re-tapped to provide a smoother surface.

Figure 7.9 Re-tapping of threads

The gaps found in the Gyroid sample were repaired using steel filled epoxy, see Figure 7.10.

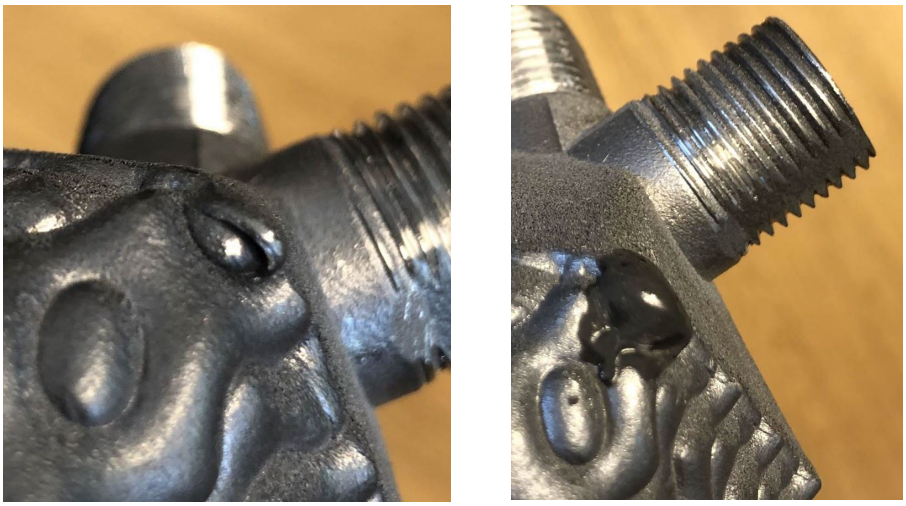

Figure 7.10 Gyroid hole and repair

7.4.6 **Leak Testing**

As all the internal channels share walls, there is no possible way for a channel to leak into itself. Leak test can therefore be done by pressurizing each flow side separately as seen in Figure 7.11. If water is seen on the outside or coming out of the other channel, a leak is present. Each channel was pressurized with tap water for 30 minutes and no detectable water was collected. Leaks smaller than visible are negligible in this situation. One centiliter per 30 minutes only accounts for around 0.00007% of the volume flow rate at 0.5 l/min, which is the lowest flow used. This is outside of the measurable range. It is also considering that the same fluid will be used in both channels and that pressure will be consistently lower during test runs.

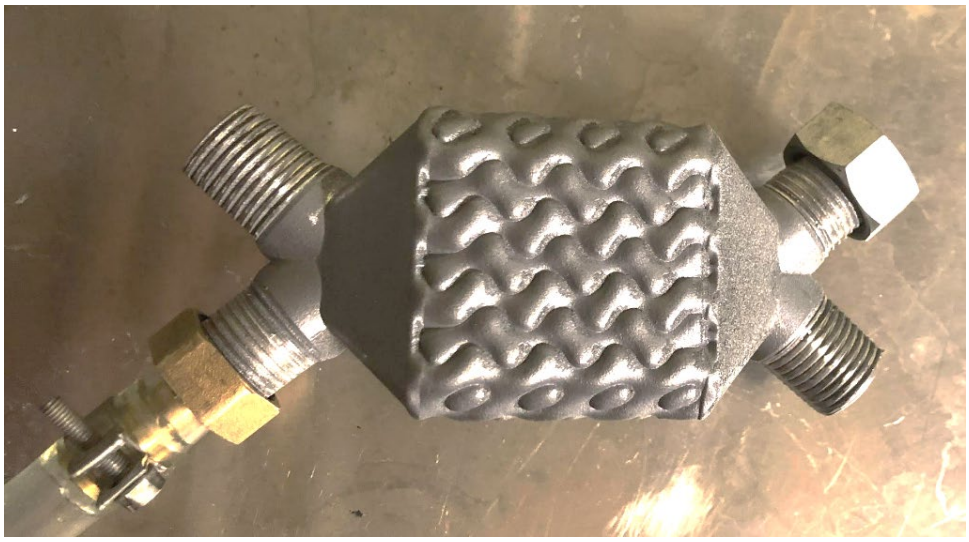

Figure 7.11 Leak test

8 Experiment and simulation

Design of experiment, experiment procedure as well as simulation parameters are presented in this chapter.

8.1 Background

A visit was conducted to the RISE facility in Mölndal, where previous samples in ReLed-3D have been tested with flowing oil. It was decided to not use the existing test rig, mainly because it is only capable of testing one flow at a time. This project requires two flows.

A HX test setup suitable for the project needs was provided by the Heat Transfer Division at the Energy Sciences Department at LTH. After consultation with Zan Wu, PhD, the decision was made to use water in both the hot and cold flow. The reason being ease of use and to avoid unnecessary safety risks introduced by use of oil.

8.2 Design of experiment

8.2.1 **Aim**

Testing of the samples will be performed with the goal of ranking among samples, and to compare our findings with the results of published research. The main questions to answer are:

- Are TPMS a suitable venue for metal AM HX?
- Which is most suitable: Diamond or Gyroid?
- What is the performance of the chosen manifold design?

8.2.2 **Principles**

The experiment must compare the three manufactured samples in a way that provides answers to above questions. To achieve comparable results, as many independent input variables as possible must be kept the same between runs making any variations depend on the samples.

The inlet temperatures are kept constant, and the same flow rates are tested for all samples. Counter current flow orientation will be used in all cases. Flow rates influence pressure drop and the nature of the flow itself. To record the changes of these, various flow rates should be tested. Both channels will have the same flow rate at any given time. This makes comparisons between flows possible.

Data recordings will be made when temperatures stabilize for a given flow rate.

Large temperature differences will make changes in temperature greater which reduces the relative contribution of reading errors. The difference between the two inlets should therefore be as big as possible.

Insulation of parts that have a temperature difference towards the surroundings will both make the experiment more reliable and reduce the heating needs of the system.

8.3 Experiment setup

The provided test rig shown in Figure 8.1 is constructed to test a heat exchanger with two liquid flows. One cold and one warm is pumped from the reservoirs shown in Figure 8.2. The flow rates are individually controlled with manual valves and displayed with flow meters. Temperature and pressure can be measured through ports at each inlet and outlet.

Figure 8.1 Test rig

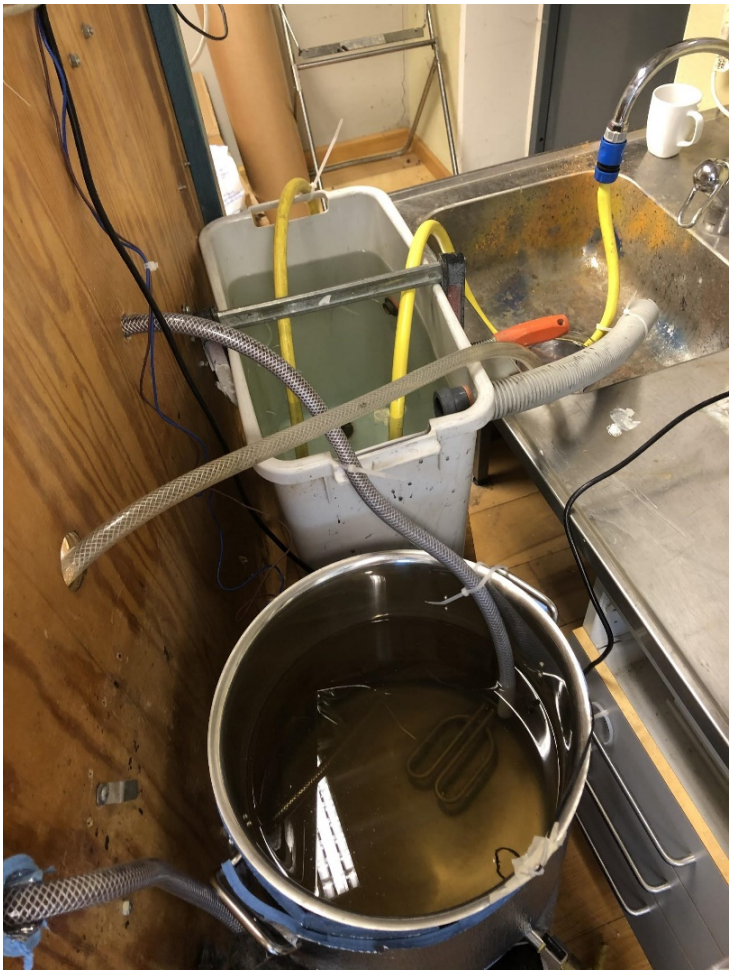

Figure 8.2 Hot and cold water reservoirs

Already assembled equipment on the rig included:

- Pumps. Two variations of Grundfos 25-60 180.
- Krohne Optiflux 1000 electromagnetic flowmeter with IFC 050 electromagnetic flow converter for the warm flow.
- Yokogawa Differential Pressure Transducer EJA110A.
- 2 x Rotameters for the cold flow (+ two additional, disconnected).
    - 1 with a heavy float to measure high volumetric flows.
    - 1 with a light float to measure low volumetric flows.
- One cold water tank, with drain and hose adapter.
- 2 x gate valve for controlling flow rate.
- Assorted piping and tubing.

Modification that were made:

- Pumps were rotated 90°. This was done to lessen the amount of trapped air, since impeller pumps are not self-priming.
- Pressure transducer was replaced with 2 x U-pipe manometers.

The equipment was supplemented with:

- Hot water tank with 2.4 kW internal heating element.
- On/off temperature control with 0.3°C hysteresis.
- Additional 2 kW induction hot plate for the hot reservoir.
- 10 mm foam insulation of the tested sample as well as the hot hoses, connectors and reservoir.
- Shelf for electric connections. Positioned such as to reduce the risk of getting hit by water in case of a leak.
- Work light.
- Assorted piping and wiring.

8.3.1 **Calibration**

All measurement equipment was calibrated to the best of our ability. Due to the indicating nature of the trials, a lower exactness is allowed. Underlying values are given in Appendix D.

8.3.1.1 Electromagnetic flow meter

The volumetric flow rate was measured to determine the need for calibration of the IFC050. The flow was set to 5 l/min and water was collected for a period of time. The collected volume was measured, and the flow rate calculated. The measured volumetric flow rate was within 2% of the Optiflux display value. Furthermore, the displayed volumetric flow was 0 when no flow was present. The previous calibration was deemed sufficiently accurate.

8.3.1.2 Rotameters

The Rotameter calibration was performed similarly to that of the electromagnetic flow meter. The relation between the rotameter float height and the volumetric flow is stated to be linear [35]. Thus, several measurements were performed at varying volumetric flows to determine the linear relation. This was repeated for both connected rotameters.

8.3.1.3 Atmospheric U-Tube differential pressure manometers

The working principle of this instrument is so reliable that no sources of error were found. No calibration was performed.

8.4 Experiment procedure

The sample being tested was mounted with the four ½" threaded connectors. Every connector has a thermocouple placed in an integrated thermo-well and a hose connecting the internal flow with the appropriate part of the U-tube manometer. The sample and the connectors were then insulated. Water in the hot reservoir was heated to 60°C and held at that temperature. Cold water was supplied from the cold reservoir, which was continuously refilled directly from the municipal supply.

Cold and hot water was pumped through the system. The cold flow was drained, and the hot flow returned to the hot reservoir, closing the loop. The globe valves were adjusted to the set flow rate. When it was judged that readings were steady, measurements were recorded for temperatures of all in- and outlets.

The manometer height difference was recorded for both flows and translated from mm water to Pascal. The temperatures were collected manually from a data logger displaying them continuously.

This was performed for 0.5 l/min and 1 – 9 l/min in increments of 1 l/min. The whole procedure was repeated for each sample.

Figure 8.3 Measurements, Comparison sample attached to test rig

8.5 Simulation

A CFD simulation was performed in collaboration with Philip Månsson, master student at LTH. Only the Gyroid was simulated. The main purpose of the simulation was to investigate that which could not be seen in the experimental testing: The distribution and motion of the internal flow. Because of this, and limited resources, the fluid motion was simulated, and heat transfer excluded.

One of the HX internal flows was isolated and placed in the software STAR CCM+. It was meshed according to Figure 8.4 and Figure 8.5. Approximately 21000000 cells were used, with special focus on the boundary layers.

Figure 8.4 Mesh

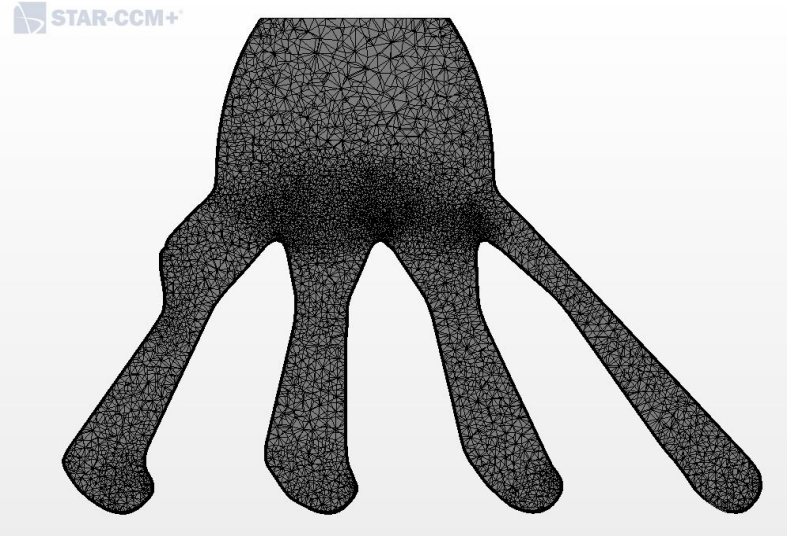

Figure 8.5 Detail

The fluid was specified as 10°C water with standard density and viscosity. Incompressibility was assumed. The fluid flow is from the top of the model, going downwards. The boundary conditions were:

- Mass flow rate at the inlet = 1.5 kg/s.
- Pressure at the outlet = 0 Pa.

The mass flow rate corresponds to 9 l/min, the highest volumetric flow rate during the experiments.

9 Results

In this chapter, results from modeling, manufacturing, experiments, and simulations are presented.

9.1 Modeling

Three samples were modeled. Figure 9.1 shows renders of the Diamond (left) and the Gyroid variation (right), with a spherical cutout to visualize the internal structure.

Figure 9.1 Renders with cut-out

The approximate dimensions of the inner structures of the CAD files are shown in Table 9.1. One manifold has 4100 mm^2 heat exchanging area, for comparison.

Table 9.1 Values of the CAD files

Concept	Heat transferring area [mm^2]	Volume [mm^3]	Compactness [m^2/m^3]
Diamond	25 400	126 600	200
Gyroid	32 300	148 900	217

9.2 Manufacturing

All samples were printed successfully and according to expectations. Figure 9.2 shows the parts in the as-built condition.

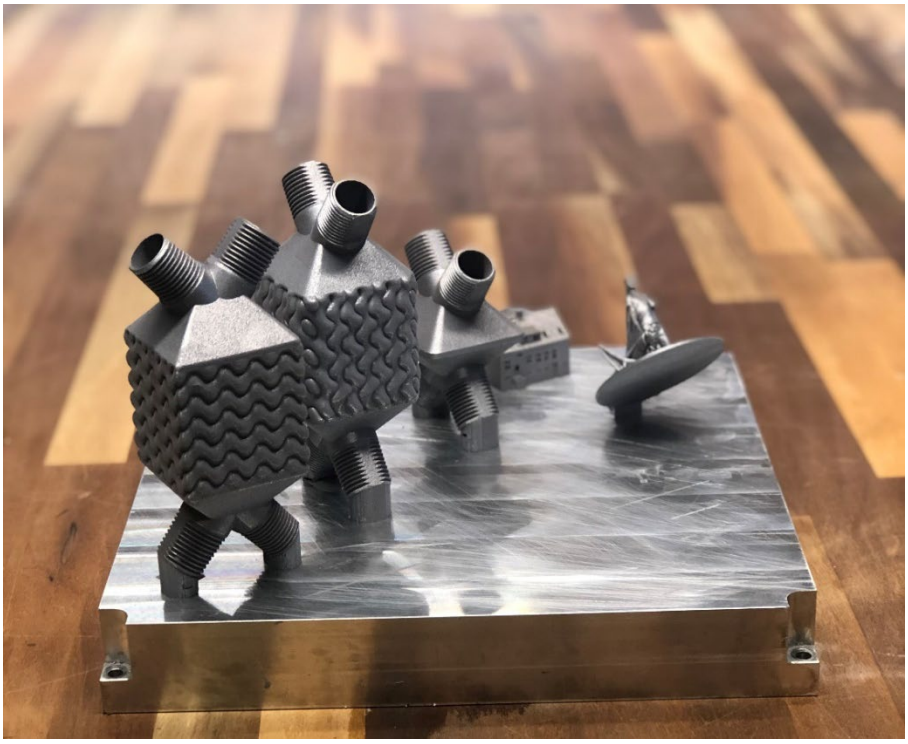

Figure 9.2 As-built parts

Print data, extracted from 3DXpert 13.0 is shown in Appendix F.

9.3 Experiment

Temperature measurement for the inlet and outlet thermocouples of both flows are consolidated in Figure 9.3 and Figure 9.4. All of the following tables are plotted against the volumetric flow rate from 0.5 to 9 l/min, and share the same legend. Full temperature readings are found in Appendix E.

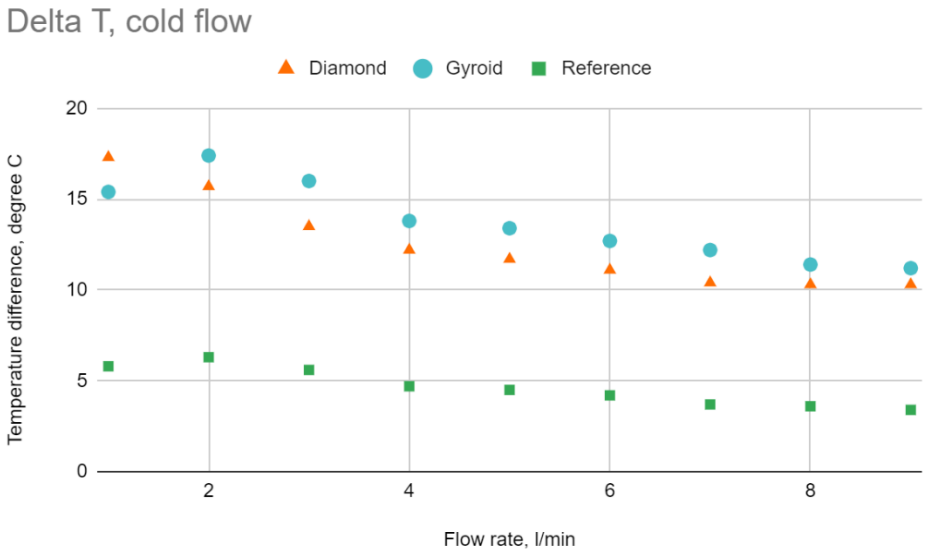

Figure 9.3 Delta T for cold flow

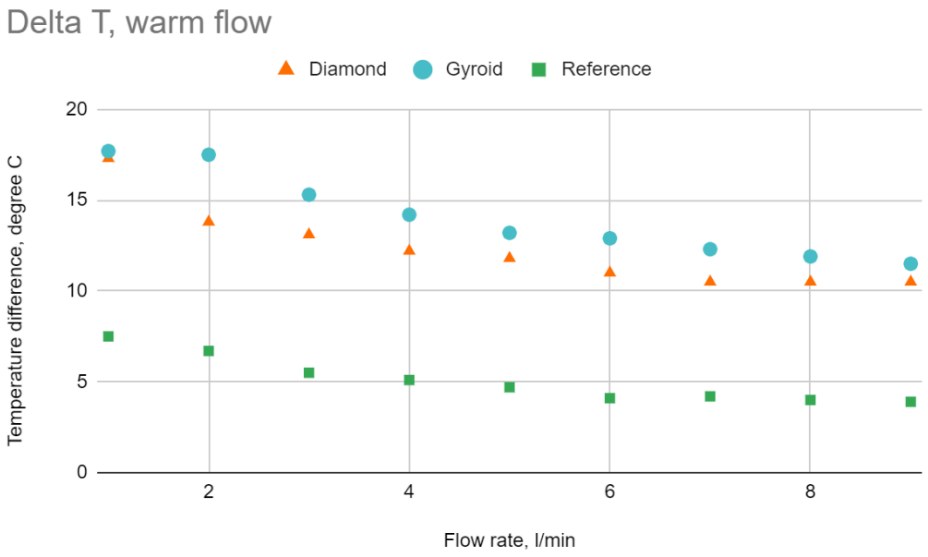

Figure 9.4 Delta T for warm flow

The recorded pressure drop for all measurements are consolidated in Figure 9.3 and Figure 9.4.

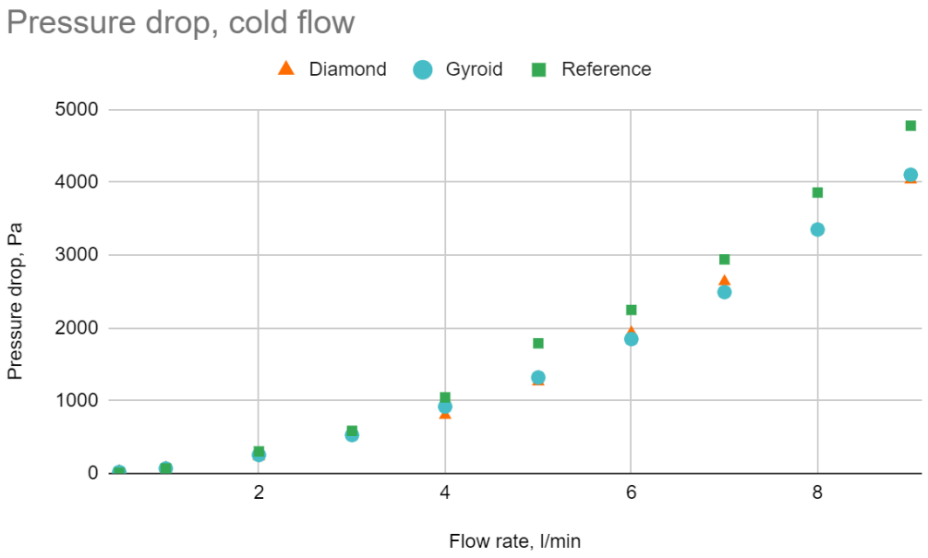

Figure 9.5 Pressure drop for cold flows

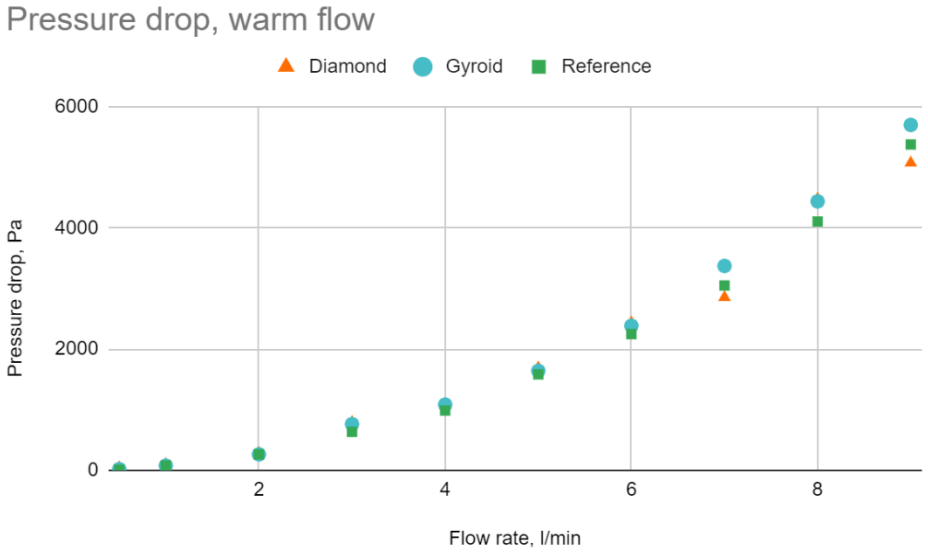

Figure 9.6 Pressure drop for warm flows

LMTD is calculated from temperatures at inlets and outlets, then overall heat transfer coefficient, as seen in Figure 9.7 was calculated according to equation (3.1) with the average of $\dot{Q}$ for the warm and cold flow.

Because water only has very small variations in density and specific heat within the temperature range of the experiment, they are estimated as constant for the calculations (995 kg/m^3 and 4200W/kg*K).

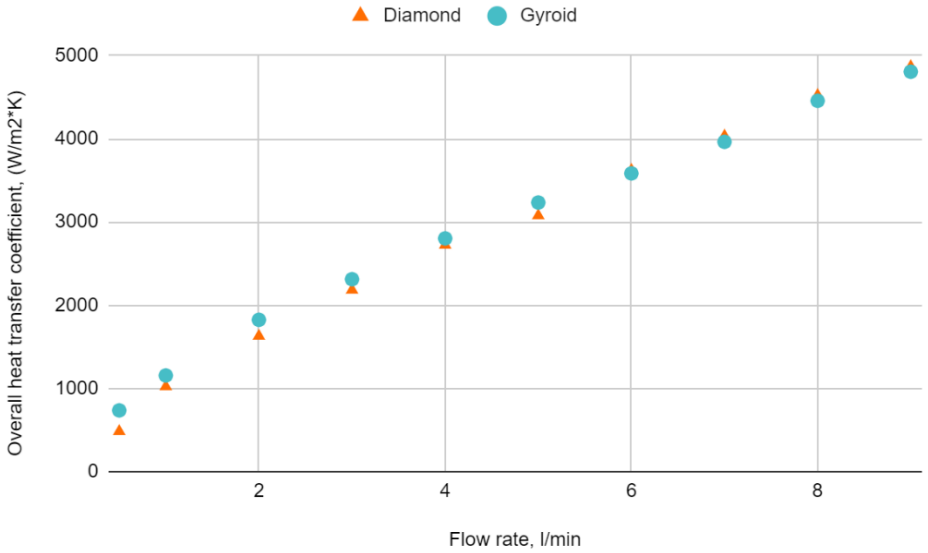

Figure 9.7 Overall heat transfer coefficient

9.4 Simulation

The flow line visualization of the performed CFD simulation is presented below in Figure 9.8, and more specified in Figure 9.9. Coloration shows the velocity of the flow in the z-direction.

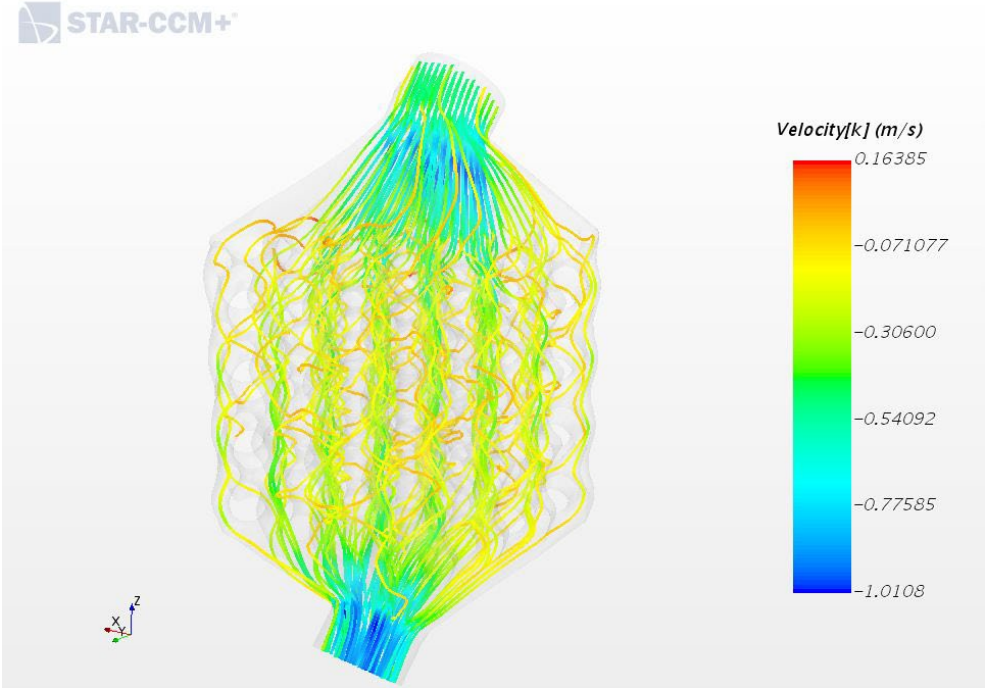

Figure 9.8 CFD visualized with flow lines

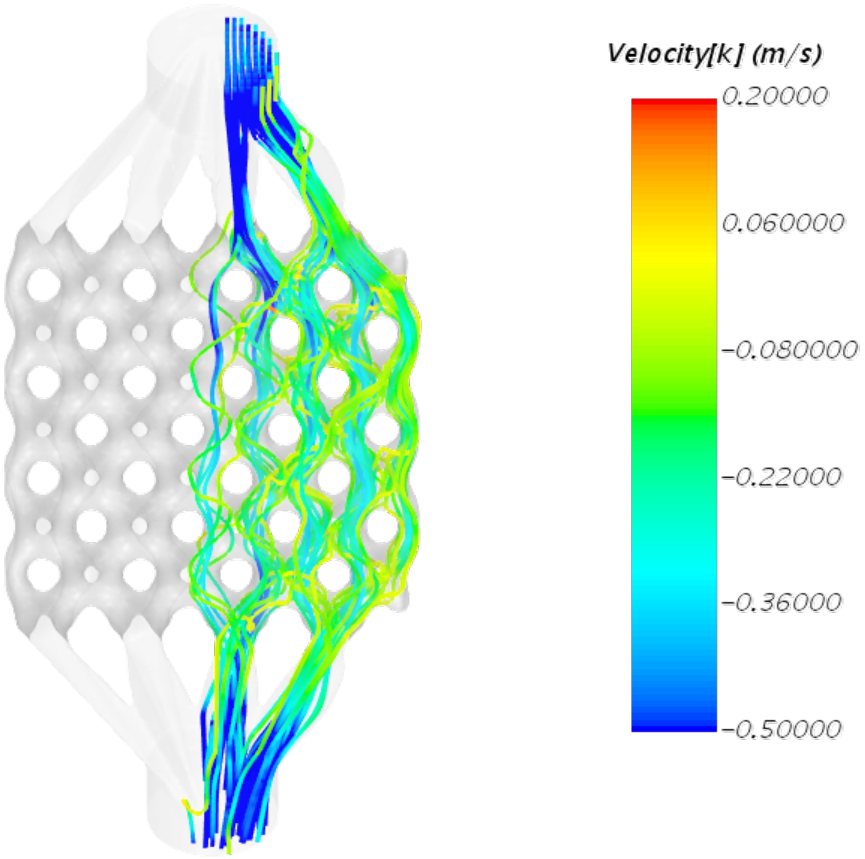

Figure 9.9 Detail of flow lines

The inlet manifold was of special interest due to its expected high contribution to pressure drop and unfavorable flow phenomena. Velocity profiles are shown in Figure 9.10 and Figure 9.11.

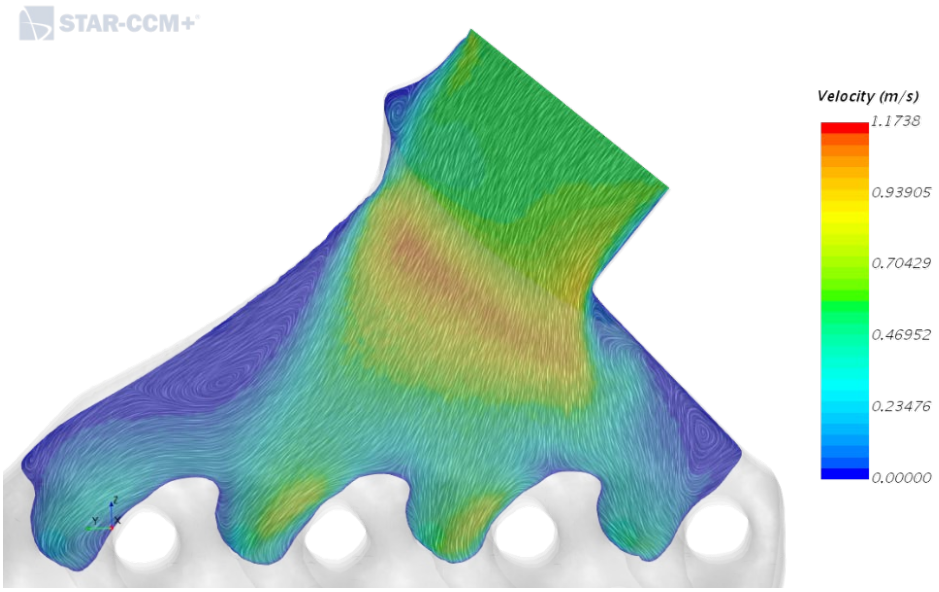

Figure 9.10 Velocity gradients in manifold

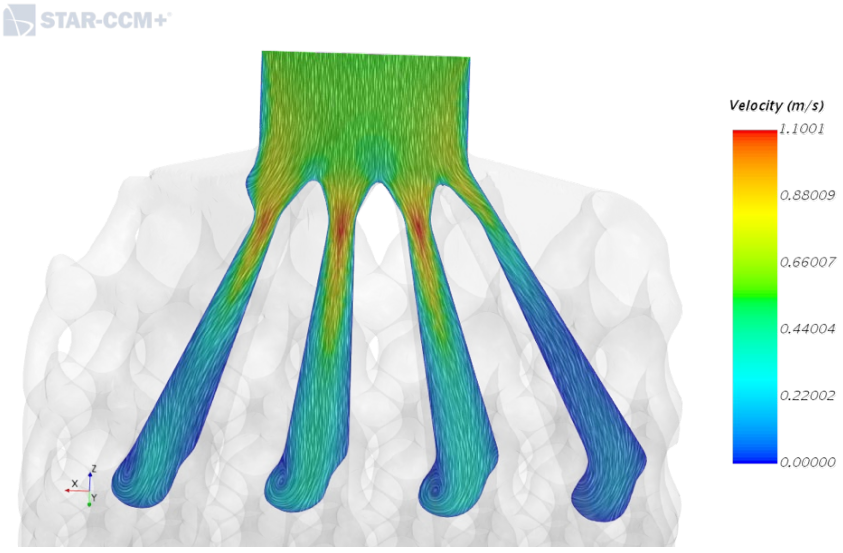

Figure 9.11 Velocity gradients in manifold, perpendicular

The flow distribution is shown with velocity profiles in Figure 9.12 at four z-heights, from the inlet and further on into the HX.

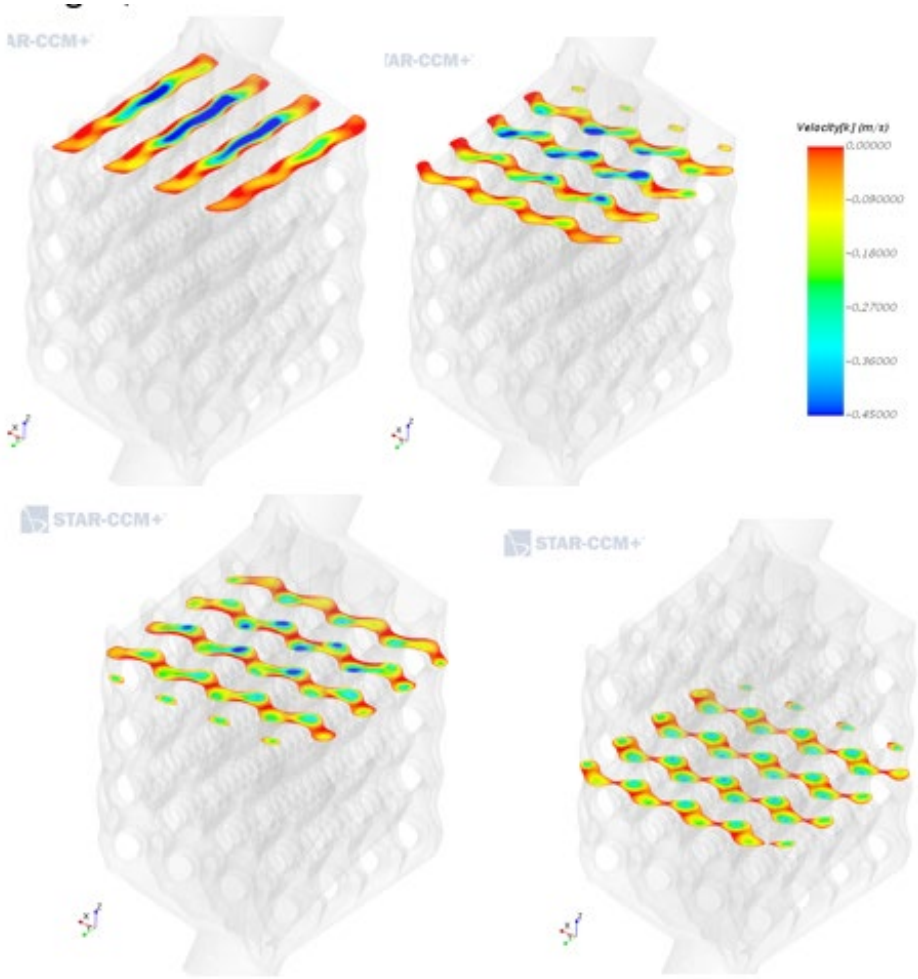

Figure 9.12 Velocity profiles

10 Discussion

Methods and results are discussed in this chapter, focusing on what has been learned throughout the whole project.

10.1 Concept selection

The scoring matrix method was altered, compared to Section 2.4. There was no score weighting. No static reference concept was used, instead the concepts were ranked compared to each other. The final scores were averaged by the contribution from each criterion.

We chose criteria that we deemed important to the performance of the HX. These criteria were hard to determine with our limited knowledge of fluid dynamics. Even though time had been spent researching the subject, our newly gained knowledge and intuition simply was not enough to rank concepts correctly. It could have been more effective to limit criteria to those which could be judged on a firmer basis.

Plastic prototypes could have been made to better gauge performance of concepts, and to catch modelling errors. This was not done mainly for two reasons. The first being that the time between printable models and deadline for production was short, and secondly because the test rig was not available at that time. Another way would have been to simulate the concepts, as was done for the final model, but at the time of concept selection CFD simulations were not available to us.

In hindsight it is very possible that another manifold concept would have performed better than the one chosen. But it is important to note that the main reason that we used a concept scoring was to finally set in stone which concept to move forward with. As a tool to reach an agreement and meet the deadline, it was successful.

10.2 Modeling

The choice of using volumetric modeling was suitable when dealing with TPMS. It allowed the trigonometric functions to be used directly and allowed the outer surface to be easily modeled.

Because prototyping and learning was performed alongside with the production of results the resulting scripts were large and ineffective. Because meshes without thickness were converted to volumes, the meshes density had to be high in order to intersect every voxel. At the same time the voxels had to be small enough to capture the small detail of the thin walls and the sharp corners in the top of the manifold channels. Decreasing the voxel side length with 50% for example results in 8 times as many voxels. The combination of these factors resulted in a very computationally intensive script. The slow response of the program hindered iteration of the designs and made errors slip through undetected.

As distance fields and distance functions were foreign and unintuitive concepts to us, we regarded the conversion of all parts into meshes as a time saver. This resulted in a modeling path with more conversions than necessary. Keeping the modeling process purely volumetric until export seems to be a promising method for organic transition between shapes and very suitable for DfAM. The similarity between the voxel volume and a powder bed volume also speaks to its advantage for AM applications [17].

10.3 Manufacturing

Two of the threads were left-handed which was due to a modelling error. The threads were mirrored instead of rotated from the original features. A mnemonic device regarding the modeling of threads was coined with inspired of this: “Threads rotate”. The Gyroid HX also had a noticeable error in two of the corners, due to a mistake in the modelling process. The connecting mesh between the manifold and the Gyroid was rotated, when it instead should have been mirrored.

These mistakes could have been avoided by using cheaper FFF to check function, model quality and scaling. This should be done for any part that is meant to fit a thread or similar feature before sending to SLM. The reasons for not doing this was because of the short timeframe between finished models and deadline for printing, and because the test rig was not available at that time.

Surface quality on the downward facing surfaces of the manifold was quite poor and on the upward facing surfaces quality was better. This was expected, and important to note is that the surface quality seen on the outside should indicate that of the inside only in “reverse”. If the manifold is rough on the outside, it is pretty on the inside. Results from ReLed3D-showed that roughness of the as-printed surface was superior with respect to heat transfer but resulted in higher pressure drop. This is probably because it introduces turbulence.

Not many examples of successfully manufactured TPMS HX were found during research. The manufactured results of this thesis is therefore considered an important contribution to the field.

10.4 Experiment

The pressure drop over the three samples are very similar at all flow rates. The differences are small enough to be contributed by inaccuracies and the fact that viscosity varies with temperature and all samples have different temperature distributions. The similarity indicates that the manifolds contribute with a dominating part of the pressure drop in the Diamond and Gyroid samples. This effect was much more pronounced than expected, and further investigation is needed to say anything conclusive.

The temperature differences recorded from the hot and cold flow are very similar, when comparing Figure 9.3 and Figure 9.4. Because the specific heat and flow rate are very similar for the two flows, similar temperature differences validates the experiment procedure. This is because of the conservation of energy.

The performance in term of transferred heat and pressure drop appear to be very similar between the Gyroid and Diamond sample. As a way of comparing the performance, both the temperature difference and the pressure drop was consolidated and plotted against the flow rate, as seen in Figure 10.1. They still appear to have very similar performance.

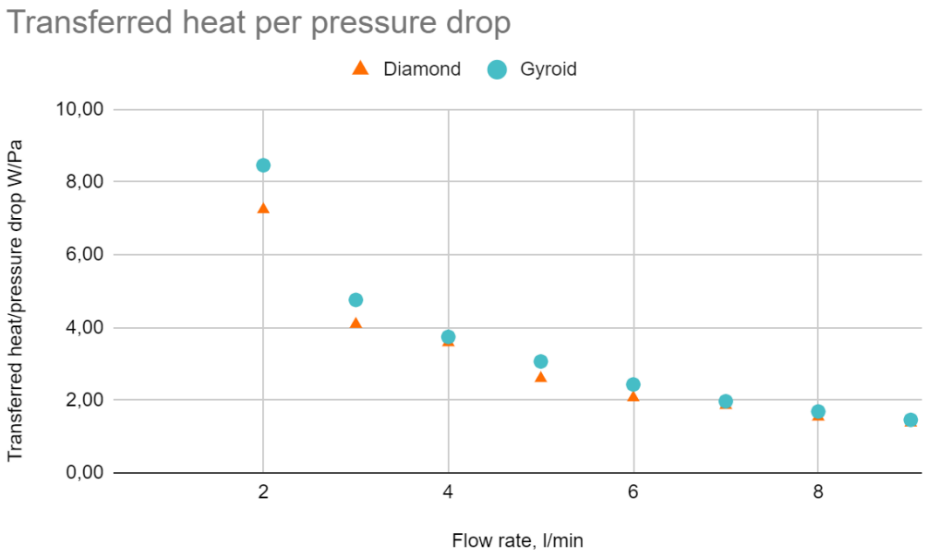

Figure 10.1 Consolidation of results

Looking at the overall heat transfer coefficient in Figure 9.7, the values of the Gyroid and the Diamond seem to converge with higher flow rates. However, the pressure drop seems to diverge with increased flow rate (see Figure 9.5, Figure 9.6).

Since the pumps could not produce higher flow rates, there was no way to produce a more conclusive result.

10.4.1 **Sources of error**

10.4.1.1 Modeling

The samples were planned to have symmetrical flows within themselves. Because of modelling errors and constrained time some asymmetry was present. To investigate the impact of this, all flow configurations should preferably be tested and compared. There was no time available for that.

The designs were planned to have the same outer dimensions to make comparison easier. Because of the modelling issues described in 10.2 the dimensions of the Gyroid and Diamond were not identical. This makes the Gyroid look more favorable in Figure 9.3 and Figure 9.4, because it has a bigger heat transferring area. The impact is reduced in Figure 9.7, because the overall heat transfer coefficient takes the area into account.

10.4.1.2 Measuring

Pressure values and flow meter values were measured manually with a ruler, introducing a certain error. The measuring devices themselves all have a certain error margin. The error margin was not calculated.

10.5 Simulation

The results of the simulation indicate:

- The flow through the inlet and outlet manifold is uneven.
- The manifold does not distribute the flow equally over the TPMS.
- The flow is more equally distributed further into the TPMS structure.
- Mixing occurs between the channels.
- Recirculation zones and boundary layer separation exist at the inlet pipe and below each connection of the Gyroid channels.

The flow seems to follow the channels all the way out to the sides. The aim of reducing dead zones and providing suitable walls seems to be successful. The experimental testing indicated that the manifolds contributed with a large part of the pressure drop of the entire HX. This is somewhat validated by the simulation results, especially regarding the impact of the inlet. The lack of a radius on the inlet pipe seems to have a large impact, as expected. The inner structure seems to equalize differences in the flow, when moving a few unit cells in. This result is consistent with results shown by Hao Peng et. al. [30].

10.6 Fluid dynamics

A big emphasis was put on symmetrical flows for in and outlet during concept generation. The effect of the outlet on the pressure drop was perhaps overestimated, when considering the simulation results. If the inlet of each flow is well designed for smooth transition into the HX, compromises can be made in the outlet design if no egregious fluid dynamic crimes are committed.

Since an AM HX can't be disassembled if made in one piece, the problem of fouling needs carefully considered. Hence, high mixing of the flows inside an AM HX is even more desirable than a conventional HX.

10.7 Time plan

Some deviations from the original time plan happened. Some of the changes that were made were intentional and reflect changes in the direction and intentions of the project. For example a test rig was originally planned to be constructed, and when this could be avoided time was directed to other activities. Some changes were due to unplanned delays. For example the concepts decision happened later than predicted. The two participants of the project put different amount of focus and time into different phases, but the overall distribution was found to be equal.

11 Conclusion

Here the conclusions are presented. They refer back to the brief posed in Section 4.4 and the questions asked in Section 8.2.1. Through summarizing and interpreting the results, it is concluded whether the brief is fulfilled, and the questions answered. Suggestions of further research marks the end of this thesis.

11.1 Are TPMS a suitable venue for metal AM HX?

This study has proven the manufacturability of the Gyroid and Diamond TPMS structures with a channel width of 6mm and a wall thickness of 0.5mm, with the material AlSi10Mg in an SLM machine. The novel outer enclosing was also manufactured successfully.

The performed experiment indicates that the inner structure contributes with a minor part of the pressure drop, compared to the manifold. Because of the complicated nature of fluid flow, this is not conclusive.

Generally it is hard to compare HX for different applications. The performance is not static, but highly dependent on operating conditions. It should also be noted that we do not have the necessary resources to do such a comparison. We have not found a reliable way to compare the performance of the manufactured samples to the examples found during research. Alas, the overall heat transfer coefficients are comparable with commercial HX [36], indicating the usefulness of both the Diamond and Gyroid sample.

The answer to the posed question is a cautious “Yes”.

11.2 Which is most suited: Diamond or Gyroid?

Because the samples have different outer dimensions, comparison is hard. But when comparing values that take this into account, as in Figure 9.7 and Figure 10.1, the performance seems to be similar. The decision must be based on other factors as well. The geometry of the Diamond structure is simpler and more symmetrical. Modelling is therefore more straight-forward, and integration of manifolds and outer walls takes less effort.

The answer is that Diamond has a slight advantage.

11.3 What is the performance of the chosen manifold?

Both experiments and simulation show that the manifold in its current design has bad flow characteristics. It does not distribute the flow very even, and it does not provide a smooth transition with a low pressure drop. The overall design is however not dismissed. It is possible that more gradual transitions between features and modifications to the proportions of the bands can make it more favorable.

The answer to this question is that more work remain, to find a suitable manifold design.

11.4 Reflection

We think that the deliverables were produced and the results are interesting. They are not conclusive, but that was expected considering the complexity and broad scope of the project. It is certain though, that more analysis of the manufactured samples would have provided better answers. Testing in other ways and with more repetitions would have been done if more time was available.

11.5 Further research

The field of AM HX can be expected to expand greatly in the near future. This thesis expands the foundation from which further research can be done. Concepts that were dismissed in this project can be further developed, and might prove successful. The samples can also be further tested and simulated in the future.

We consider the developed method of encapsulating the inner channels a valuable and concrete result to be integrated into future work. We believe that the general

concept of TPMS in HX is very promising to pursue in combination with AM. The resistance to high operating pressures and temperatures are interesting avenues to explore.

One can imagine the inner structure of a TPMS to be gradually scaled and skewed over the length of the HX, providing optimal conditions throughout the volume. The structure can be modified to provide its own manifold, integrated in the TPMS channel network. An example of such a manifold was designed, after the presented samples were manufactured. It is shown in Figure 11.1, where the Diamond structured is gradually scaled in each step through the structure.

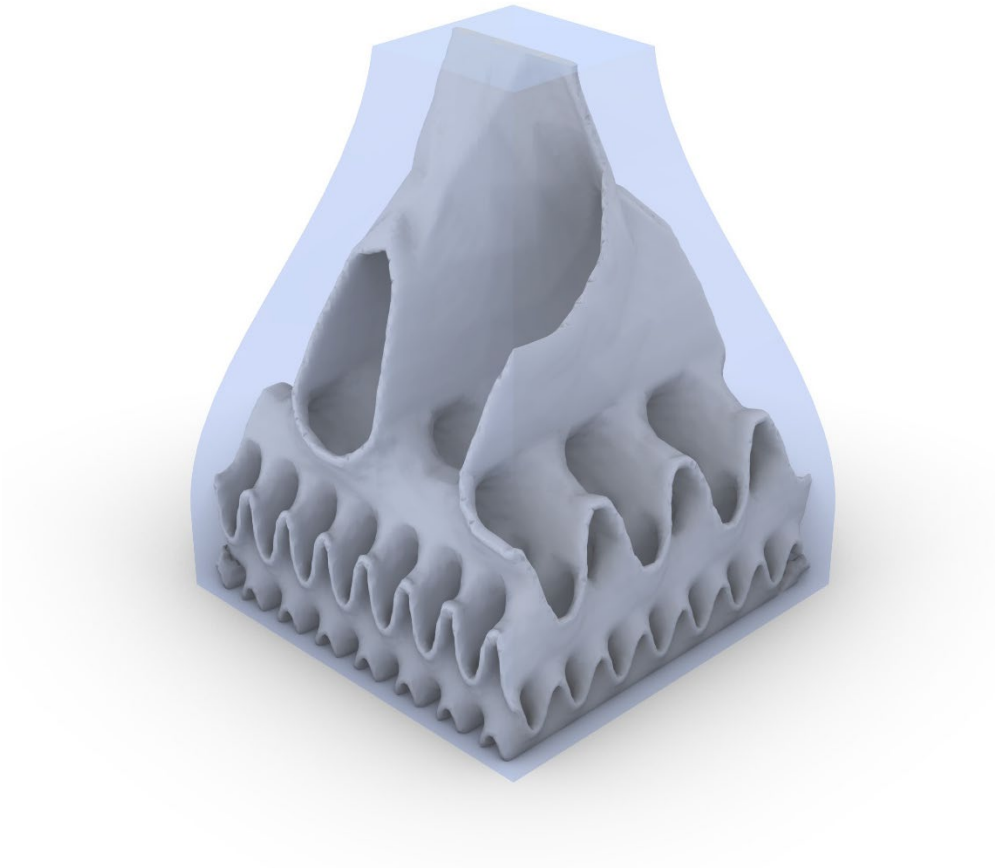

Figure 11.1 Modified Diamond TPMS manifold

The whole HX should be volumetrically modeled without conversions along the way. If this design workflow is connected with CFD simulations and optimizations are performed we believe that a very promising concept is found.

References

[1] O. Diegel, A. Nordin and D. Motte, A Practical Guide to Design for Additive Manifacturing, Springer eBooks, 2019.

[2] Design Council, "Eleven lessons: managing design in eleven global brands," [Online]. Available: https://www.designcouncil.org.uk/sites/default/files/asset/document/Eleven Lessons_Design_Council%20(2).pdf. [Accessed 25 May 2020].

[3] K. T. Ulrich and S. D. Eppinger, Product Design and Development, 5th Ed. ed., New York: McGraw-Hill, 2012.

[4] S. Davidson, "Grasshopper," 2020. [Online]. Available: https://www.grasshopper3d.com/. [Accessed 28 05 2020].

[5] 3D Systems, "ProX DMP 320," 2016. [Online]. Available: https://www.3dsystems.com/press-releases/3d-systems-launches-prox-dmp-320-high-precision-high-throughput-direct-metal-printing.

[6] B. Sundén, Introduction to Heat Transfer, Southampton: WIT Press, 2012.

[7] "www.ge.com," General Electric, 2020. [Online]. Available: https://www.ge.com/additive/additive-manufacturing/information/3d-printing. [Accessed 28 05 2020].

[8] 3D Systems, "Direct Metal Printing Design Guide," 2019. [Online]. Available: https://www.3dsystems.com/definitive-guide-metal-printing-landing-page. [Accessed 29 April 2020].

[9] I. Y. Anik, "ISO/TC 261 Additive Manufacturing," 2011. [Online]. Available: https://www.iso.org/committee/629086.html. [Accessed 28 05 2020].

[10] Y. Z. J. L. T. Z. A. A. A. Arfan Majeed, "Investigation of T4 and T6 heat treatment influences on relative density and porosity of AlSi10Mg alloy components manufactured by SLM," *Computers & Industrial Engineering,* vol. 139, no. https://doi.org/10.1016/j.cie.2019.106194, 2020.

[11] G. V. V. Juan Asensio-Lozano, "Tech notes The Al-Si Phase Diagram," 2015. [Online]. Available: https://www.buehler.com/assets/solutions/technotes/vol5issue1.pdf. [Accessed 28 05 2020].

[12] L. A. L. Pedersen, "The effect of solution heat treatment and quenching rates on mechanical properties and microstructures in AlSiMg foundry alloys," *Metall and Mat Trans,* vol. 32, no. https://doi.org/10.1007/s11661-001-0069-y, p. 525–532, 2001.

[13] GPI Prototype and manufacturing services, "Material data sheet, EOS aluminium AlSi10Mg," [Online]. Available: https://gpiprototype.com/pdf/EOS_Aluminium_AlSi10Mg_en.pdf. [Accessed 28 05 2020].

[14] G. T. M. S. Y. Z. Ç. Ö. Ö. S. Y. A. M. C. E. K. Gökhan Özer, "Investigation of the effects of different heat treatment parameters on the corrosion and mechanical properties of the AlSi10Mg alloy produced with direct metal laser sintering," *Materials and Corrosion,* vol. 71, no. https://doi.org/10.1002/maco.201911171, 2019.

[15] L. A. D. D. R. B. D. K. S. J. D. C. Pin Yang, "Microstructure evolution and thermal properties of an additively manufactured, solution treatable AlSi10Mg part," *Joirnal of Material Research,* vol. 33, no. https://doi.org/10.1557/jmr.2018.405, pp. 4040-4052, 2018.

[16] J. Ljungman, 3D-Printed Heat Exchanger, Lund: Department of Design Sciences, 2019.

[17] M. Bernhard, M. Hansmeyer and B. Dillenburger, "Volumetric modelling for 3D printed architecture," *Advances in Architectural Geometry,* pp. 392-415, 2018.

[18] R. K. K. N. M. F. E. M. H. J. A. G. G. a. D. L. Uwe Scheithauer, "Advances in Heat Exchangers," in *Potentials and Challenges of Additive Manufacturing Technologies for Heat Exchanger*, 2018.

[19] General Electric, "GE Research launches project to develop metal additively manufactured heat exchanger," 24 April 2019. [Online]. Available: https://www.3dnatives.com/en/ge-research-heat-exchanger-240420195/. [Accessed 28 05 2020].

[20] K. G. S. C. J. H. Brandon J.Hathaway, "Design and characterization of an additive manufactured hydraulic oil cooler," *International Journal of Heat and Mass Transfer,* vol. 117, no.

https://doi.org/10.1016/j.ijheatmasstransfer.2017.10.013, pp. 188-200, 2018.

[21] Y. H. R. R. Zhiwei Huang, "Review of nature-inspired heat exchanger technology," *International Journal of Refrigeration,* vol. 78, no. https://doi.org/10.1016/j.ijrefrig.2017.03.006, pp. 1-17, 2017.

[22] M. R. E. Adrian Bejan, "Deterministic Tree Networks for Fluid Flow: Geometry for Minimal Flow Resistance Between a Volume and One Point," *World Scientific,* vol. 05, no. https://doi.org/10.1142/S0218348X97000553, pp. 685-695, 1997.

[23] P. C. Yongping Chen, "Heat transfer and pressure drop in fractal tree-like microchannel nets," *International Journal of Heat and Mass Transfer,* vol. 45, no. 13, pp. 2643-2648, 2002.

[24] M. F. E. D. L. Kevin NOACK, "COMPLEX HEAT EXCHANGERS –THE COMBINATION OF FRACTAL GEOMETRY AND ADDITIVE MANUFACTURING," *Journal of Industrial Design and Engineering Graphics,* vol. 14, no. 1, 2019.

[25] K. N. D. L. Martin Friedrich Eichenauer, "Mixing of Fluids with Space-Filling Curves," *Advances in Intelligent Systems and Computing,* pp. 1255-1267, 2019.

[26] T. V. Oevelen, "Numerical Topology Optimization of Heat Sinks," in *International Heat Transfer Conference*, 2014.

[27] C. B. D. D. R. F. O. S. B. S. L. Sumer B. Dilgen, "Density based topology optimization of turbulent flow heat transfer systems," *Structural and Multidiciplinary Optimization,* vol. 57, pp. 1905-1918, May 2018.

[28] A. J. M. W. TimFemmera, "Estimation of the structure dependent performance of 3-D rapid prototyped membranes," *Chemical Engineering Journal,* vol. 273, pp. 438-445, 1 August 2015.

[29] J. K. Stolaroff, "FEW0233: Additive Manufacturing of New Structures," in *Crosscutting Research Program Portfolio Review Meeting*, 2018.

[30] F. G. W. H. Hao Peng, "DESIGN, MODELING AND CHARACTERIZATION OF TRIPLY PERIODIC MINIMAL SURFACE HEAT EXCHANGERS WITH ADDITIVE MANUFACTURING," in *30th Annual International Solid Freeform Fabrication Symposium – An Additive Manufacturing Conference*, 2019.

[31] M. C. Escher, Artist, *Metamorphosis III.* [Art]. 1968.

[32] Morphcode, "Intro to L-systems," 2013. [Online]. Available: https://morphocode.com/intro-to-l-systems/. [Accessed 28 05 2020].

[33] A. L. Przemyslaw Prusinkiewicz, The Algorithmic Beauty of Plants, New York: Springer-Verlag, 1990.

[34] R. M. Dickau, "Two-Dimensional L-systems," July 1997. [Online]. Available: http://mathforum.org/advanced/robertd/lsys2d.html. [Accessed 28 05 2020].

[35] Z. Wu, Interviewee, *Ph D.* [Interview]. 06 05 2020.

[36] Alfa Laval, "The theory behind heat transfer," [Online]. Available: https://www.alfalaval.com/globalassets/documents/microsites/heating-and-cooling-hub/alfa_laval_heating_and_cooling_hub_the_theory_behind_heat_transfer.pdf. [Accessed 28 05 2020].

[37] Design guidelines 3dsystems.

Appendices
Appendix A Project plan, original

Project plan for master thesis: “Development of 3D printed heat exchanger and test rig”

Performed by Isak Wadsö and Simon Holmqvist, 31/1-2020 → 12/6-2020 at Lund Technical University

0768-955506 isak.wadso@gmail.com, 0735-857698 mas15sho@student.lu.se

Supervised by Axel Nordin and Martin Andersson

axel.nordin@design.lth.se, Martin.Andersson@energy.lth.se

Background

Heat exchangers are used to heat or cool fluids in countless applications such as air conditioning, process industry, power generation and in vehicles. Much work has been done on optimization, and even small improvements in heat transfer, pressure drop or size are considered successes.

Since traditional manufacturing methods put constraints on the design freedom, additive manufacturing (3D printing) in metal holds the promise for big advancements. It can create very complex internal structures that might give higher performance, and to use only one material throughout the product can prevent leakage and allow for higher operation temperatures. Furthermore it adds the flexibility to make changes from unit to unit and to customize its outer shape. All of this in a single manufacturing step. But AM also has its own limitations. Physical tests needs to be done, as both production and operation of these products are hard to simulate.

What we know about heat exchangers has to be reevaluated, and there are many new aspects to explore. Much research is now being done in this area.

This thesis is part of the project "ReLed-3D, Resource efficient flexible production in the automotive industry through additive metal manufacturing", funded by VINNOVA FFI – Strategic Vehicle Research and Innovation. The demonstration part for the project is an oil cooler in a Volvo truck. Previous findings from the

ReLed-3D project such as generated concepts, test results, print parameters, simulation model etc. will be used in this thesis.

Objective

The goal of this master thesis is to widen the understanding of what can be achieved with heat exchangers, by exploring the possibilities of additive manufacturing. The thesis will be oriented to best suit the authors' education and strengths, which involves the vision to find interdisciplinary possibilities combined with a rapid prototyping approach (Think-Try-Change).

The thesis will consist of two main parts:

The test rig available in the project will be reconstructed. It currently only support one fluid circuit, so another one has to be added in order to get closer to emulate real operation. It will be used to test printed samples designed in this thesis and further on in the project.

Concepts for new geometries suitable for AM will be explored and compared. Because organic, irregular and complicated shapes are now possible, inspiration will be sought in nature. Examples will be manufactured based on the design guidelines found previously in the project, and then evaluated in the test rig.

To be able to get quick feedback from testing, changing between prototypes needs to be fast. The test rig should limit minimal macro structure design regarding design of inlets and outlets, to allow a large variety of designs. The test rig should measure pressure drop and temperature change between both inlets and outlets. It should have a reliable and adjustable flow rate.

With respect to the geometry design, these areas are of initial interest:

The conditions of the real world application of the heat exchanger and how this should affect the macro level design

- Exploring overall concepts possible with AM
- Bio mimicking solutions for heat transfer and flow manipulation
- How the meso structure should facilitate high heat transfer and low pressure drop. Are there any unexplored avenues to achieve a good balance?
- Compliant mechanism applications for flow manipulation
- Support structure utilization

The aim is to develop a geometry that is in alignment with the ReLed-3D project goals of reducing the size and weight of the HX, and improving the heat exchange. This can be achieved by focusing on the macro level design, optimizing macro geometry for the real world use case and implementing meso level designs from previous phases of the ReLed-3D project. Another possible route to the same goal is to test previous and new meso structures with a set, general macro design.

Improving both meso and macro structure at the same time will introduce uncertainties in the interpretation of results, i.e. it is bad design of experiments.

Method

The project will follow this general structure:

1. Clarifying the scope and goals of the project
2. Gather and process information
3. Generate concepts for heat exchanger and test rig designs
4. Compare and choose concepts
5. Develop the chosen concepts
6. Testing and verification
7. Delivery of results in a report, a presentation and physical prototype

This process has a structure similar to the "double diamond" method. It will also have the structure of two parallel projects during the phases 3-6.

The initial phase of the degree project will consist of information gathering and processing. First, articles concerning progress in the ReLed-3D project will be studied. Then books and articles about heat transfer, heat exchanger design, additive manufacturing and other areas of interest will be studied. Information will also be gathered from conversations with experts. A visit to the RISE research facility in Mölndal where previous testing has been done will be conducted.

Next, the generation of concepts will start along with designing the test rig. Since the test rig put constraints on the geometry, it needs to be finished before designs are printed. Basic simulations can be used during the geometry design process to affirm or deny design decisions. Plastic SLS printing may also be used for intermediate prototypes. Further development will be carried out based on test results and iterated to confirm any improvement if present.

A thesis, a presentation and physical prototypes will be the deliverables of this degree project. Methods, process and results are recorded throughout the degree project and will be consolidated in the thesis. It will describe the steps taken and reasoning behind decisions and form the basis for the presentation.

Conditions

The objective is to conduct many tests in combination with rapid prototyping. Focus will be on exploring the macro and meso geometry. The micro geometry is outside of the scope. Since Isak and Simon study Technical Design, advanced CFD simulations will be avoided due to the time needed to master this field.

The work will be performed at IKDC in Lund. Office space and workshops will be provided here, as well as access to the SLM and SLS machines that will be used. Access to computers and programs such as Ansys, Solidworks and Rhino Grasshopper are provided by the university.

Support and consultation will mainly be provided by Axel Nordin. Since he is engaged in the ReLed-3D project, regular meetings will be held to keep each other informed. Meetings with assistant supervisor Martin Andersson will be held as needed, when questions regarding thermodynamic and fluid dynamics arise and in cases when detailed simulations are needed. Contacts in the ReLed-3D project will be acquired as needed to gain insights from their experiences.

Further limitations and clearer goals will be established as the degree project progresses.

Time plan

A plan is established, that map out the project's phases and checkpoints. It is not static, but a tool to guide the work which means it will be subject to changes as the project progresses.

Appendix B Project plan, revised

Project plan for master thesis: “Development and testing of 3D printed heat exchanger”

Performed by Isak Wadsö and Simon Holmqvist, 31/1-2020 → 12/6-2020 at Lund Technical University

0768-955506 isak.wadso@gmail.com, 0735-857698 mas15sho@student.lu.se

Supervised by Axel Nordin and Martin Andersson

axel.nordin@design.lth.se, martin.andersson@energy.lth.se

Background

Heat exchangers are important devices used to heat or cool fluids in countless applications such as air conditioning, process industry, power generation and in vehicles.

Traditional production methods put many constraints on the design of heat exchangers. Applying additive manufacturing (AM) allows for more complex geometries, which holds the promise of improved heat transfer. It can produce a finished product in a single manufacturing step in a variety of materials including metals and ceramics. Customization is also possible.

Immature technology and high price have hindered this development, but now it is rapidly getting explored. One promising concept for AM heat exchangers is to use a class of structures known as “triply periodic minimal surface”(TPMS). They form two intertwined 3-dimensional channel patterns, providing large surface area and good mixing. Some work has been done on designing a complete heat exchangers based on these structures, but making full use of the possibilities with AM is still an open field.

This thesis is part of the project "ReLed-3D, Resource efficient flexible production in the automotive industry through additive metal manufacturing", funded by VINNOVA FFI – Strategic Vehicle Research and Innovation. The demonstration part for the project is an oil cooler in a Volvo truck.

Objective

The goal of this project is to explore the possibilities of aluminum AM heat exchangers, resulting in a robust, adjustable and parametric 3D model in Rhino Grasshopper. It aims to fulfill the goals of the ReLed-3D project: Reduction in size and weight of the current heat exchanger, and improved heat transfer. Optimization of this geometry, with respect to fluid dynamics, is considered outside the scope.

It has a vision to find interdisciplinary connections and will use a rapid prototyping approach (Think-Try-Change).

The project will consist of two main parts:

- Geometries will be explored, developed and printed.
- The samples will be experimentally tested. Pressure drop and temperature difference will be measured during operation.

The focus will be to integrate a TPMS structure, appropriate in- and outlets and a suitable outer casing. Additional aspects of the geometric design include:

- Using the full potential of AM
- Support structure utilization
- The conditions of the real world application of the heat exchanger
- Bio mimicking solutions for heat transfer and flow manipulation
- The combination of meso and macro level structures

Method

The project will follow this general structure:

1. Clarifying scope, goals and delimitations
2. Gather and process information
3. Generate concepts for heat exchanger
4. Compare and choose concepts
5. Develop the chosen concepts
6. Collect and analyze test data
7. Delivery of results: Report, presentation and prototypes

This process has a structure similar to the “double diamond” method.

The initial phase of the degree project will consist of information gathering. First, articles concerning progress in the ReLed-3D project will be studied. Then books and articles about heat transfer, heat exchanger design, additive manufacturing, TPMS and other areas of interest will be studied. Information will also be gathered from conversations with experts. A visit to the RISE research facility in Mölndal where previous testing has been done will be conducted.

Next, the generation of concepts will start. Basic simulations can be used during the geometry design process to affirm or deny design decisions. Plastic SLS printing may also be used for intermediate prototypes. Geometries will be compared and evaluated. One or more of the most promising versions will be printed in aluminum.

The sample/s will be evaluated regarding pressure drop and temperature difference with the equipment at the Department of Fluid Dynamics at LTH.

If time is available, further development will be carried out and iterated based on the test results.

A thesis, a presentation and physical prototypes will be the deliverables of this degree project. Methods, process and results are recorded throughout the degree project and will be consolidated in the thesis. It will describe the steps taken and reasoning behind decisions and form the basis for the presentation.

Conditions

Previous findings from the ReLed-3D project such as generated concepts, test results, print parameters, simulation model etc. will be used in this thesis.

The macro and meso geometry will be explored, while the micro geometry is outside of the scope. Since Isak and Simon study Technical Design, Extensive 3D modelling will be performed. Advanced CFD simulations will be avoided due to the time needed to master this field.

The work will be performed at IKDC in Lund. Office space and workshops will be provided here, as well as access to the SLM and SLS machines that will be used. Access to computers and programs such as Ansys, Solidworks and Rhino Grasshopper are provided by the university.

Support and consultation will mainly be provided by Axel Nordin. Since he is engaged in the ReLed-3D project, regular meetings will be held to keep each other informed. Meetings with assistant supervisor Martin Andersson will be held as needed, when questions regarding thermodynamic and fluid dynamics arise and in cases when detailed simulations are needed. Additional contacts in the ReLed-3D project as well as outside will be acquired.

Time plan

A plan is established, that map out the project's phases and checkpoints. It is not static, but a tool to guide the work which means it will be subject to changes as the project progresses.

Appendix C Time plan

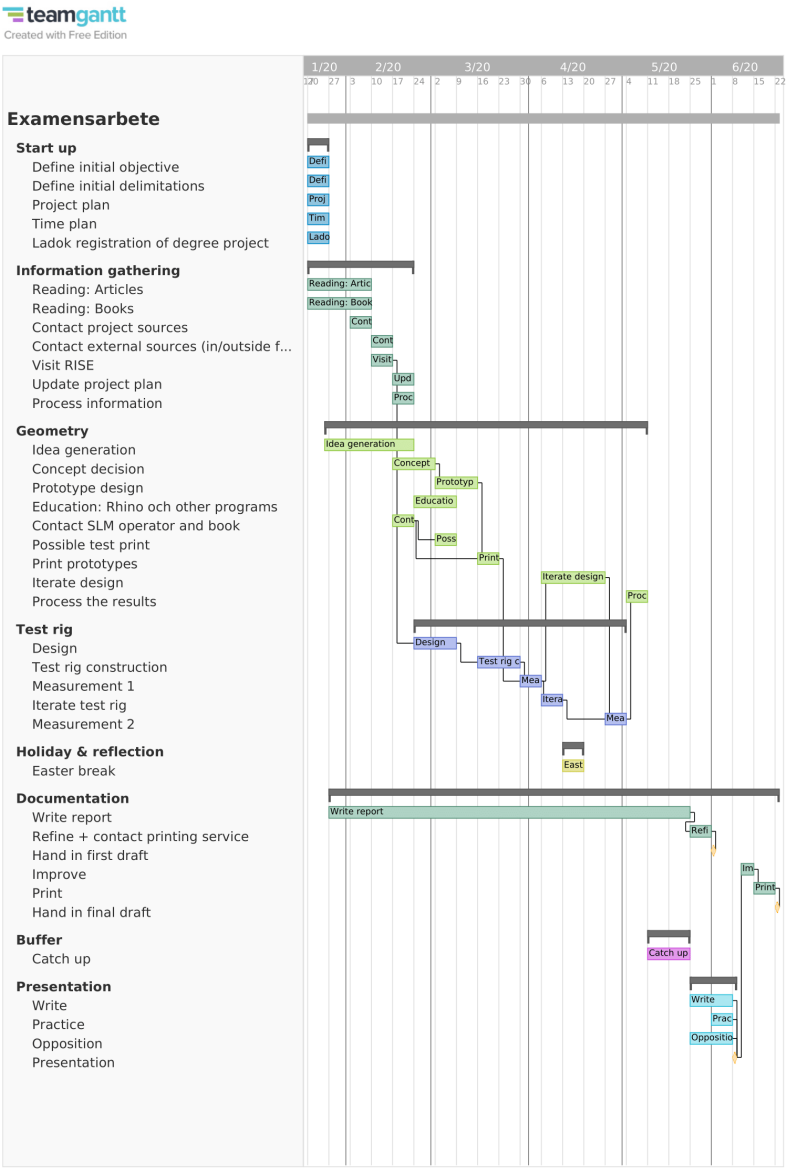

Appendix D Calibration values

Big flowmeter value	Meassured volume [l]	time [min]	time [s]	Calculated flow (l/min)
5	7.5	2.003	120.18	3.74
3	4.75	2.209666667	132.58	2.15
7.8	15.1	2.5125	150.75	6.01
11.2	9.05	1.007	60.42	8.99
small flowmeter value				
6.8	0.905		120	0.45
27.5	2.98		120	1.49
46.5	3.12		69	2.71

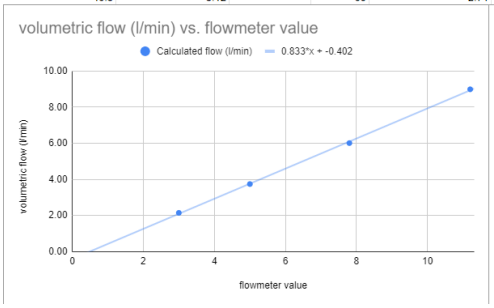

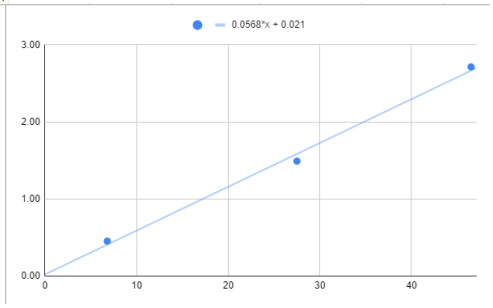

Optiflux calibration check				
time [min]	vol [l]	vol. flow [l/min]	Optiflux display value	
1.368833333	7.05	5.150371362	5.05	OK
		1.020	0.020	
		0.981	0.019	

Thermocouple readings after long equiliberation				
Date	T1	T2	T3	T4
14/5	21.1	21	20.7	21
--	20.9	20.8	20.5	20.9
--	20.9	20.8	20.7	20.9
18/5	20.5	20.5	20.5	20.5
--	20.6	20.6	20.6	20.6
Average:	20.80	20.74	20.60	20.78
20.6	0.20	0.14	0.00	0.18

Appendix E Temperature readings

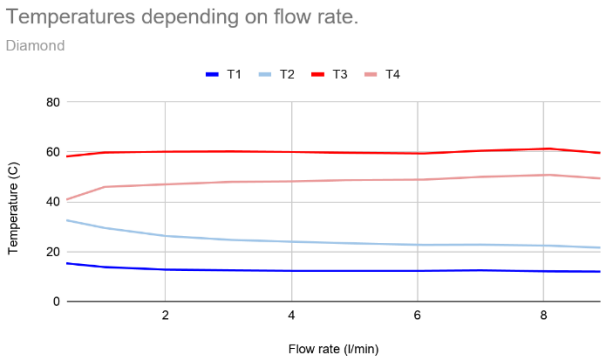

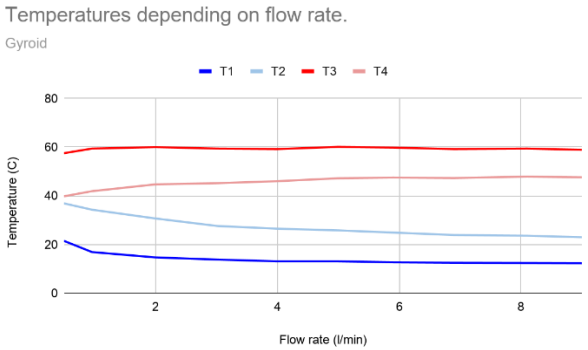

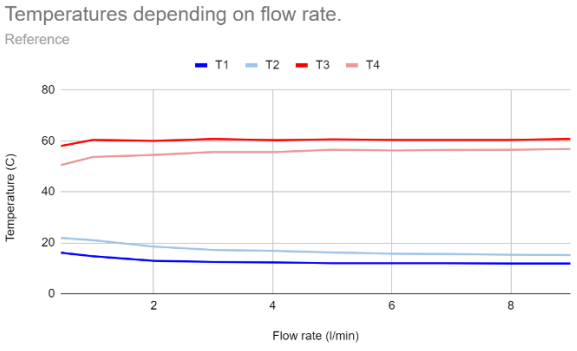

Appendix F Print time

	Diamond	Gyroid	Comparison
Material incl. supports [cm^3]	64.77	69.25	25.48
Scanning time excl. supports (hh:mm:ss)	04:36:48	05:46:45	02:03:25
Time between Layers (hh:mm:ss)	02:38:29	02:35:06	01:37:22

Total build time amounted to 30h 41min.